

Chromatic spherical invariant and Hennings invariant of 3-dimensional manifolds

J. Reina¹

¹Univ Bretagne Sud, CNRS UMR 6205, LMBA, F-56000, Vannes, France, email : julie.reina@univ-ubs.fr

Abstract

This paper establishes a relation between two invariants of 3-dimensional manifolds: the chromatic spherical invariant \mathcal{K} and the Hennings-Kauffman-Radford invariant HKR. We show that, for a spherical Hopf algebra H , the invariant \mathcal{K} associated to the pivotal category of finite-dimensional H -modules is equal to the invariant HKR associated to the Drinfeld double $D(H)$ of the same Hopf algebra.

Contents

1	Introduction	1
2	Hopf algebra's definition	3
2.1	Hopf algebras and integrals	3
2.2	Drinfeld double	6
3	Computation of the HKR invariant	8
4	The chromatic spherical invariant \mathcal{K}	9
4.1	Virtual Heegaard diagrams	9
4.2	The map F'' over virtual Heegaard diagrams	15
4.3	The chromatic spherical invariant \mathcal{K}	22
5	Relation between invariants	29
6	References	39

1 Introduction

It was long conjectured and progressively established until recently (in [TV17]) that there exists a connection between the Witten–Reshetikhin–Turaev invariants and the Turaev–Viro construction. Both of these constructions fundamentally rely on the semi-simplicity of the underlying tensor category. The Hennings–Kauffman–Radford invariant, denoted HKR, and the Kuperberg invariant, denoted Kup, are often regarded as

non-semisimple counterparts of the Witten–Reshetikhin–Turaev invariant and the Turaev–Viro construction, respectively. In the non-semisimple setting, it has been analogously conjectured that the Kuperberg invariant Kup , associated to a finite-dimensional Hopf algebra H , is related to the invariant HKR defined using the Drinfeld double of H , $D(H)$. Since the formulation of this conjecture, several partial results have been established supporting this relation.

The work presented in this paper has been motivated by the article [CC19], in which Chang and Cui proved that, for a finite-dimensional double balanced Hopf algebra H and a closed oriented 3-manifold M , there exists a framing b and a 2-framing ϕ of M such that

$$\text{Kup}(M, b; H) = \text{HKR}(M, \phi; D(H)).$$

In [CGPMT20], Constantino, Geer, Patureau-Mirand, and Turaev introduced the spherical chromatic invariant \mathcal{K} and proved that, for any finite-dimensional involutive pivotal unimodular unibalanced Hopf algebra H , there is equality between the invariant $\mathcal{K}_{H\text{-mod}}$ and the Kuperberg invariant associated to H for any connected closed oriented 3-manifold.

In this article, we provide an explicit algorithm for computing the invariant of connected closed oriented 3-manifold $\mathcal{K}_{H\text{-mod}}$, for any finite-dimensional spherical Hopf algebra H . To this end, we introduce a new type of diagram, which we call *virtual Heegaard diagrams*. These are a variant of classical Heegaard diagrams that allow for crossings on the β -curves.

This computational method enables us to establish the following restricted version of the conjectured relation mentioned above.

Theorem 1.1 (Main Theorem). *Let H be a spherical Hopf algebra and M be a 3-dimensional closed connected oriented manifold. Then,*

$$\mathcal{K}_{H\text{-mod}}(M) = \text{HKR}_{D(H)}(M),$$

where $D(H)$ denotes the Drinfeld double of H and $H\text{-mod}$ is the pivotal category of finite-dimensional H -modules.

The invariant $\mathcal{K}_{\mathcal{C}}$ is defined for a pivotal category \mathcal{C} , and likewise, the HKR invariant has been generalized for categories by Lyubashenko. Both invariants can be viewed as induced by a ribbon TQFT (see [DRGG⁺22] and [CGPMV23] respectively). A similar result to this article was established in [MSWY23] in the setting of representations of diffeomorphism groups. In their work, Müller, Schweigert, Woike, and Yang use string-nets to construct a modular functor $\text{SN}_{\mathcal{C}}$ from a pivotal category \mathcal{C} (it is suspected [MSWY23, Rk 2.17] that this functor extends into the TQFT of [CGPMV23]). They also prove [MSWY23] that the functor $\text{SN}_{\mathcal{C}}$ of a finite pivotal tensor category is equivalent to Lyubashenko’s modular functor associated to the Drinfeld center of that category. We suspect the existence of a similar relation between the $(2 + 1)$ -TQFT of [DRGG⁺22] and that of [CGPMV23].

The first part of this article establishes the conventions we will use for Hopf algebras and their Drinfeld doubles. We then describe computational methods for the HKR invariant and for the invariant \mathcal{K} . This will include the definition of virtual Heegaard diagrams and the algorithm for computing $\mathcal{K}_{H\text{-mod}}$ using them. In the final part of the paper, we state and prove our main result, establishing the relationship between the two invariants discussed before.

Acknowledgments : The author wants to thank Bertrand Patureau-Mirand for his guidance and advice throughout the research and writing of this article. The author also wishes to thank François Constantino and Nathan Geer for their insights that aided in the research for this article. This work was partially funded by the France 2030 program, Centre Henri Lebesgue ANR-11-LABX-0020-01.

2 Hopf algebra's definition

2.1 Hopf algebras and integrals

We begin by establishing the conventions on Hopf algebras that will be used throughout this work.

Let $H = (H, \eta, m, \epsilon, \Delta)$ be a finite-dimensional Hopf algebra over a field \mathbb{k} , with bijective antipode S , and unit map $\eta : \mathbb{k} \rightarrow H$ defining the unit element $1_H := \eta(1) \in H$. For every $n \in \mathbb{N}$, we denote by $\Delta^{(n)} : H \rightarrow H^{\otimes n}$ the iteration of the coproduct defined recursively by $\Delta^{(0)} = \epsilon$, $\Delta^{(1)} = \text{Id}_H$ and $\Delta^{(n+1)} = (\text{Id}^{\otimes(n-1)} \otimes \Delta) \circ \Delta^{(n)}$ for $n \geq 1$. We will always use Sweedler's notation for the coproduct,

$$\Delta^{(n)}(x) = x_{(1)} \otimes \cdots \otimes x_{(n)} \quad (1)$$

that hides the summation symbol.

A map f will occasionally be written as $f(\varphi)$, where φ denotes the argument. We denote by $\tau : H \otimes H \rightarrow H \otimes H$ the map : $a \otimes b \mapsto b \otimes a$.

We recall some standard definitions on Hopf algebras (see [Rad11] and [GHPM22] for more details).

Definition 2.1. • A right (resp. left) *integral* on H is an element $\lambda \in H^*$ such that

$$\lambda(x_{(1)})x_{(2)} = \lambda(x)1_H \quad (\text{resp. } x_{(1)}\lambda(x_{(2)}) = \lambda(x)1_H),$$

for all $x \in H$.

• A left (resp. right) *cointegral* in H is an element $\Lambda \in H$ such that

$$x\Lambda = \epsilon(x)\Lambda \quad (\text{resp. } \Lambda x = \epsilon(x)\Lambda),$$

for all $x \in H$.

• A *group-like* element in H is an element $g \in H$ satisfying $\Delta(g) = g \otimes g$ and $\epsilon(g) = 1$.

It follows from the definition that a group-like element g is invertible and satisfies $S(g) = g^{-1}$.

Definition 2.2. • Let Λ be a nonzero left cointegral of H . There exists a group-like element $\alpha \in H^*$ determined by the relation

$$\Lambda v = \alpha(v)\Lambda,$$

for all $v \in H$. We call α the *H-distinguished group-like element of H^** .

• Let λ be a nonzero right integral of H . There exists a group-like element $a \in H$ determined by the relation

$$f\lambda = f(a)\lambda,$$

for all $f \in H^*$. We call a the *H-distinguished group-like element of H* .

Since H is finite-dimensional, there is a unique (up to a scalar) right integral and left cointegral. Therefore, the distinguished group-like elements α and a are independent from the choice of Λ and λ . From now on, we fix a right integral $\lambda \in H^*$ and a left cointegral $\Lambda \in H$ such that $\lambda(\Lambda) = 1$.

Definition 2.3. A Hopf algebra H is said to be *unimodular* if it is finite-dimensional and if left cointegrals are also right cointegrals.

Remark : Saying that H is unimodular is equivalent to having $\alpha = \epsilon$.

Remark : [Rad11] If H is unimodular, then λ is a quantum character, i.e., $\lambda(xy) = \lambda(S^2(y)x)$ for all $x, y \in H$. In particular, $\lambda \circ S^2 = \lambda$.

Definition 2.4. • A Hopf algebra H with antipode S is called *pivotal* with pivot $g \in H$ if g is a group-like element such that $\forall x \in H, S^2(x) = gxg^{-1}$.

• A Hopf algebra is called *spherical* if it is pivotal and unimodular (hence finite-dimensional), with its pivot g satisfying $g^2 = a$.

Remark : In the spherical case, we have the equality $\lambda \circ S = \lambda(g^2\varphi)$ (direct consequence of [Rad11, Th. 10.5.4]).

Definition 2.5. A *symmetrized integral* in a pivotal Hopf algebra H is a linear form μ satisfying:

1. $(\mu \otimes g)\Delta(x) = \mu(x)1_H$ for all $x \in H$,
2. $\mu(xy) = \mu(yx)$ for all $x, y \in H$,
3. $\mu(S(x)) = \mu(x)$ for all $x \in H$.

Proposition 2.6. Let H be a spherical Hopf algebra and λ a right integral. Then the linear form $\mu \in H^*$ defined by $\mu := \lambda(g\varphi)$ is a symmetrized integral.

Proof. For all $x \in H$, by the definition of a right integral, we have

$$\mu(x)1_H = \lambda(gx)1_H = \lambda((gx)_{(1)})(gx)_{(2)} = \lambda(gx_{(1)})gx_{(2)} = (\mu \otimes g)\Delta(x).$$

Thus, equality 1. is verified.

In the unimodular case, by properties of right integrals and the definition of g as the pivot, for all $x, y \in H$ we have

$$\mu(xy) = \lambda(gxy) = \lambda(S^2(y)gx) = \lambda(gyx) = \mu(yx)$$

Thus, equality 2. is verified.

Since g is group-like, in particular $S(g) = g^{-1}$ and $S(g^{-1}) = g$. Therefore, for all $x \in H$, we have

$$\mu(S(x)) = \lambda(gS(x)) = \lambda(S(xg^{-1})) = \lambda(g^2xg^{-1}) = \lambda(gx) = \mu(x),$$

due to the properties of right integrals in the unimodular and spherical case. Thus, equality 3. is verified. \square

From now on, we will consider the symmetrized integral defined by $\mu := \lambda(g\varphi)$.

Definition 2.7. A Hopf algebra H is called *quasitriangular* if it admits an invertible element $R \in H \otimes H$, denoted $R = \sum_{i=1}^n r_i \otimes s_i$, satisfying

1. $\sum_{i=1}^n \Delta(r_i) \otimes s_i = \sum_{i,j=1}^n r_i \otimes r_j \otimes s_i s_j$,
2. $\sum_{i=1}^n r_i \otimes \Delta(s_i) = \sum_{i,j=1}^n r_j r_i \otimes s_i \otimes s_j$,
3. $\tau \circ \Delta(h)R = R\Delta(h)$.

This element R is called the R -matrix of H . To alleviate the notations, we will sometimes leave the summation implicit and write $R = r \otimes s$ (or $R = r_i \otimes s_i$ to keep track of the pairing between r and s when multiple iterations of R appear).

The element $u := \sum_{i=1}^n S(s_i)r_i \in H$ is called the Drinfeld element. It is invertible and satisfies, for all $h \in H$, $S^2(h) = uhu^{-1}$ and $uS(u) = S(u)u \in Z(H)$.

Definition 2.8. A quasitriangular Hopf algebra H is called *ribbon* if it admits an element $\theta \in Z(H)$, called the ribbon element, satisfying the following equations

$$\theta^{-2} = uS(u), \quad S(\theta) = \theta, \quad \epsilon(\theta) = 1, \quad \Delta(\theta) = \left(\sum_{i,j} s_j r_i \otimes r_j s_i \right) (\theta \otimes \theta).$$

The algebra is then pivotal with pivot element $g = u\theta$ (more details in the proof of [Rad11, Prop 12.3.6]).

An equivalent definition in the case of a pivotal structure is given as follows (see [GHPM22]).

Definition 2.9 (Equivalent definition, [GHPM22]). A quasitriangular pivotal Hopf algebra H is called *ribbon* if the element $\theta := m(\tau((g \otimes 1_H)R))$ satisfies

$$\theta = m((1_H \otimes g^{-1})R).$$

Remark : Since $(S \otimes S)(R) = R$, this definition is equivalent to requiring that θ satisfies $S(\theta) = \theta$.

Proposition 2.10. *An unimodular, quasitriangular, pivotal Hopf algebra H is ribbon if and only if it is spherical.*

Proof. If a Hopf algebra H is unimodular, then $a = uS(u^{-1})$, with a the distinguished group-like element of H (see [Rad11, Th 12.3.3.b]).

Let us define $\theta := m(\tau((g \otimes 1_H)R))$. Then it can be seen that $u = \theta^{-1}g$, and thus, that $\theta \in Z(H)$.

Let us assume that H is ribbon. Since $\theta = S(\theta)$ and g is a pivot for H , we compute

$$a = uS(u^{-1}) = S(u^{-1})u = \theta g \theta^{-1} g = g \theta \theta^{-1} g = g^2.$$

Thus, H is spherical.

Conversely, let us assume that H is spherical. Then,

$$\begin{aligned} uS(u^{-1}) &= \theta^{-1}g^2S(\theta) \\ \iff a &= \theta^{-1}g^2S(\theta) \\ \iff \theta g^2 &= g^2S(\theta) \\ \iff g^2\theta &= g^2S(\theta) \\ \iff \theta &= S(\theta) \end{aligned}$$

Thus, H is ribbon. □

Example of a spherical Hopf algebra:

The small quantum group $U_q = U_q(\mathfrak{sl}(2))$ (with q a $2r$ -th root of unity) is the algebra generated by E, F, K, K^{-1} together with the relations:

$$K^r = 1, \quad E^r = F^r = 0, \quad (r \in \mathbb{N})$$

$$KK^{-1} = K^{-1}K = 1,$$

$$KE = q^2EK, \quad KF = q^{-2}FK,$$

$$[E, F] = \frac{K - K^{-1}}{q - q^{-1}}$$

The following theorem gives its structure as a vector space. (A demonstration of this theorem and more details about U_q can be found in [Kas95].)

Theorem 2.11 (Poincaré-Birkhoff-Witt).

The set $\{K^m E^n F^l\}_{m,n,l \in \{0, \dots, r-1\}}$ is a basis of U_q .

The following relations give U_q a structure as a Hopf algebra.

$$\Delta(K) = K \otimes K, \quad \Delta(K^{-1}) = K^{-1} \otimes K^{-1}$$

$$\Delta(E) = 1 \otimes E + E \otimes K, \quad \Delta(F) = K^{-1} \otimes F + F \otimes 1,$$

$$\epsilon(E) = \epsilon(F) = 0, \quad \epsilon(K) = \epsilon(K^{-1}) = 1,$$

$$S(K) = K^{-1}, \quad S(K^{-1}) = K, \quad S(E) = -EK^{-1}, \quad S(F) = -KF.$$

Furthermore, it can be seen that $S^2(x) = KxK^{-1}$, thus, $g = K$ can be chosen as pivot of U_q .

Let $c \in \mathbb{k}$ be an invertible constant, a right integral of U_q is defined, on the previously mentioned basis of U_q , by

$$\lambda(KE^{r-1}F^{r-1}) = \frac{r}{c}, \quad \text{and} \quad \lambda(K^m E^n F^l) = 0 \text{ si } (m, n, l) \neq (1, r-1, r-1)$$

and a cointegral Λ is given by

$$\Lambda = c \left(\frac{1}{r} \sum_{j=0}^{r-1} K^j \right) E^{r-1} F^{r-1}.$$

We can note that $\lambda(\Lambda) = 1$ (more details in [CGHPM23]).

From λ , we get the symmetrized integral μ , defined by

$$\mu(E^{r-1}F^{r-1}) = \frac{r}{c}, \quad \text{and} \quad \mu(K^m E^n F^l) = 0 \text{ si } (m, n, l) \neq (0, r-1, r-1).$$

2.2 Drinfeld double

We consider the finite-dimensional Hopf algebra $H^{*,\text{cop}}$ defined from H by $H^{*,\text{cop}} := (H^*)^{\text{cop}} = (H^*, {}^t\epsilon, {}^t\Delta, {}^t\eta, {}^t m^{\text{op}})$ with antipode ${}^t(S^{-1})$. Here, ${}^t m^{\text{op}}$ is the map defined by $(m^{\text{op}}(f))(x \otimes y) = f(yx)$, for all $f \in H^*$ and all $x, y \in H$. The map ${}^t\Delta : H^* \otimes H^* \rightarrow H^*$ is defined through the identification $(H \otimes H)^* = H^* \otimes H^*$ by $({}^t\Delta(f \otimes g))(x) = f(x_{(1)}) \otimes g(x_{(2)})$, for all $x \in H$ and all $f, g \in H^*$.

Structure on $D(H)$: Following the conventions of [CC19] and [Rad11], the Drinfeld double $D(H) = H^{*\text{cop}} \otimes H$ of a finite-dimensional Hopf algebra H is a quasitriangular Hopf algebra with the structure given below.

For all $f \in (H^*)^{\text{cop}}$ and all $v \in H$, we have

$$1^D = \epsilon \otimes 1_H, \quad \epsilon^D = 1_H \otimes \epsilon, \quad \Delta^D = (f_{(1)} \otimes x_{(1)}) \otimes (f_{(2)} \otimes x_{(2)}),$$

$$M^D(f \otimes v, f' \otimes v') = (f f' (S^{-1}(v_{(3)}) \lrcorner v_{(1)}) \circ \Delta \otimes v_{(2)} v'),$$

$$S^D(f \otimes v) = M^D(\epsilon \otimes S(v), f \circ S^{-1} \otimes 1) = f \circ S^{-1}(v_{(3)}) \lrcorner S(v_{(1)}) \otimes S(v_{(2)}).$$

Let (e_1, \dots, e_n) be a basis of H and (e_1^*, \dots, e_n^*) the dual basis of $H^{*\text{cop}}$, we can make explicit the R -matrix of $D(H)$ by

$$R^D := \sum_{i=1}^n (\epsilon \otimes e_i) \otimes (e_i^* \otimes 1_H)$$

and its inverse by

$$(R^D)^{-1} := \sum_{i=1}^n (\epsilon \otimes S(e_i)) \otimes (e_i^* \otimes 1_H).$$

From now on, we denote the multiplication in the double by $(f \otimes v)(f' \otimes v') := M^D(f \otimes v, f' \otimes v')$. It can be noted, by direct calculation, that $(f \otimes 1_H)(f' \otimes v') = f f' \otimes v'$ and $(f \otimes v)(\epsilon \otimes v') = f \otimes v v'$, for all $(f \otimes v), (f' \otimes v') \in D(H)$.

Proposition 2.12. [Rad11, Th 13.2.1] *The Drinfeld double $D(H) = H^{*\text{cop}} \otimes H$ of a finite-dimensional Hopf algebra H is an unimodular Hopf algebra (for it is both quasitriangular and factorizable).*

As with the structure maps of $D(H)$, we can define a right integral and a $D(H)$ -distinguished group-like element based on those previously established on H ,

$$\lambda^D := \Lambda \otimes \lambda \quad \text{and} \quad a^D = \alpha \otimes a,$$

(see [CC19, Part. 2.4] and [Rad11, Part 13.7]).

Lemma 2.13. [Rad11, Lemma 13.7.2] *Let H be a finite-dimensional Hopf algebra over a field \mathbb{k} , and let a and α be the H -distinguished and H^* -distinguished group-like elements, respectively. Then, for any pair $(\beta, b) \in H^* \times H$ such that*

- β and b are group-like elements,
- $\beta^{-2} = \alpha$, $b^{-2} = a$, and
- $S^2(h) = b^{-1}(\beta(h_{(1)})h_{(2)}\beta^{-1}(h_{(3)}))b$, for all $h \in H$,

the element $(\beta \otimes b)^{-1}$ is a pivot of $D(H)$.

When H is spherical (and so, unimodular), we have $\alpha = \epsilon$ and $g^2 = a$. Therefore, the following proposition can be deduced from the lemma.

Proposition 2.14. *Let H be a spherical Hopf algebra with g as its pivot. Then its Drinfeld double $D(H)$ is also spherical with $g^D := \epsilon \otimes g$ as its pivot.*

Proof. First, let us show that the pair (ϵ, g^{-1}) satisfies the assumptions of Lemma 2.13.

By definition, g and ϵ are group-like, therefore, g^{-1} also is. Since H is spherical and unimodular, we have that $\alpha = \epsilon$ and $g^2 = a$.

It remains to verify that $S^2(h) = g(\epsilon^{-1}(h_{(1)})h_{(2)}\epsilon(h_{(3)}))g^{-1}$ for all $h \in H$. However, by the definition of ϵ and of the pivot g , we have

$$g(\epsilon^{-1}(h_{(1)})h_{(2)}\epsilon(h_{(3)}))g^{-1} = ghg^{-1} = S^2(h),$$

for all $h \in H$. Therefore, $g^D = (\epsilon \otimes g^{-1})^{-1}$ can be set as pivot of $D(H)$.

As mentioned earlier, by direct calculation we have $(\epsilon \otimes g^{-1})(\epsilon \otimes g) = \epsilon \otimes 1_H$. Therefore $(\epsilon \otimes g^{-1})^{-1} = \epsilon \otimes g$.

Furthermore, since H is spherical, we note that

$$(g^D)^2 = (\epsilon \otimes g)(\epsilon \otimes g) = \epsilon \otimes g^2 = \epsilon \otimes a = a^D.$$

Thus, $D(H)$ is also spherical. □

We can argue similarly that, if a pair $(\beta, b) \in H^* \times H$ as described in Lemma 2.13 exists, then $D(H)$ with the pivot $\beta^{-1} \otimes b^{-1}$ is spherical.

Remark : Proposition 2.14 allows us to express a symmetrized integral of $D(H)$ through elements of H and H^* .

$$\mu^D = \lambda^D(g^D \heartsuit) = \Lambda \otimes \mu$$

Remark : Since the Drinfeld double of a Hopf algebra is unimodular and quasitriangular (see [Rad11, Th 13.2.1]), Propositions 2.10 and 2.14 imply that the double of a spherical Hopf algebra is also ribbon.

3 Computation of the HKR invariant

Let M be a 3-dimensional manifold and L an oriented surgery link of M . Let H be a finite-dimensional ribbon Hopf algebra with pivot g , and μ a symmetrized non-degenerate integral of H (i.e. $\mu(g\theta)\mu(g^{-1}\theta^{-1}) \neq 0 \in \mathbb{k}$). We denote $\delta := \mu(g\theta) \in \mathbb{k}$. In the rest of this article, we assume that μ is renormalized such that $\mu(g\theta)\mu(g^{-1}\theta^{-1}) = 1 \in \mathbb{k}$. Therefore, we will use the HKR invariant with the computational algorithm described in [GHPM22] that we express as follows.

- Let D be a planar diagram of L with each component admitting a base point. For each cap, cup, and crossing, we place on D the beads described in Figure 1. Each bead is colored by an element of the algebra H . Furthermore, we denote $R = r \otimes s$.
- Starting from the base point and following the orientation, we multiply all beads in one element, which gives an element of H for each component. (All multiplications are performed from the left.) This produces an element $PT(D) \in H^{\otimes n}$ (with n the number of components of L) which we call the total bead of D (at this point, it is not an invariant of the diagram).
- The HKR invariant is given by the following theorem.

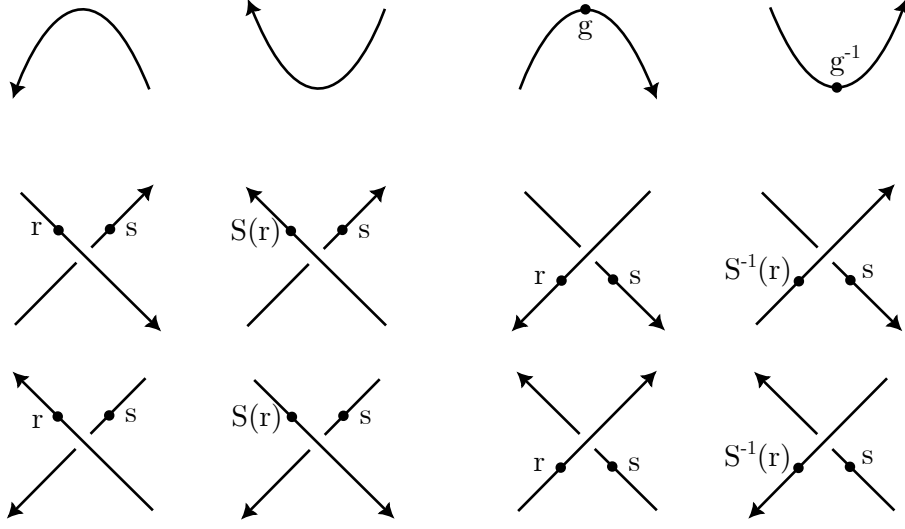


Figure 1: Beads placement (according to the conventions of [GHPM22])

Theorem 3.1. [GHPM22, Th 2.9] Let H be a finite-dimensional Hopf algebra. For each manifold M , the scalar $\text{HKR}_H(M)$ is a manifold invariant defined as

$$\text{HKR}_H(M) := \delta^{-s} \mu^{\otimes n}(PT(D)) \in \mathbb{k}$$

where D is a diagram of a surgery link of M , $s \in \mathbb{Z}$ is the signature of the linking matrix of L and n is the number of components of L .

This theorem provides a reformulation of the 3-manifold invariant introduced by Hennings [Hen96] and by Kauffman and Radford [KR95]. A proof can be found in [GHPM22, Th 2.9] considering $G = \{0\}$.

Remark : The beads on the rightmost crossing in the Figure 1 are denoted r_i and $S(s_i)$ instead of $S^{-1}(r_i)$ and s_i as in other references (see [GHPM22, Part. 2.2]). Both conventions are equivalent because $(S \otimes S)(R) = R$.

4 The chromatic spherical invariant \mathcal{K}

In this section, we fix H to be a spherical Hopf algebra over a field \mathbb{k} .

4.1 Virtual Heegaard diagrams

Next, we will define what we will call *virtual Heegaard diagrams*. Roughly speaking, these are Heegaard diagrams allowing intersection points over the β curves.

We assume that all mentioned curve are oriented.

Definition 4.1 (Heegaard diagrams). We call *Heegaard diagram* a triplet $D = (\Sigma_g, \alpha, \beta)$ such that

- Σ_g is a closed oriented surface of genus $g \in \mathbb{N}$.
- $\alpha = (\alpha_1, \dots, \alpha_g)$ is a collection of g simple closed disjoint curves.

- $\beta = (\beta_1, \dots, \beta_g)$ is a collection of g simple closed disjoint curves.
- The complement of α and the complement of β in Σ_g are connected.
- Every intersection between two curves is transverse.

In this article, we choose to consider the curves in a Heegaard diagram as oriented, although this is not usually the case in the literature on Heegaard diagrams.

Every Heegaard diagram defines a 3-manifold by gluing together two handlebodies determined by the sets of curves α and β , with boundary the surface Σ_g (more details in [OS04, Part 2]). Our interest in these diagrams stems from the following classical result (see [OS04, Theorem 2.1 and Remark 2.6]).

Theorem 4.2. *Every oriented closed 3-manifold admits a Heegaard diagram.*

In this article, we define and use a more general and abstract type of diagram encompassing Heegaard diagrams.

Definition 4.3 (Virtual Heegaard diagrams). We denote by D_{He}^v the set of triplets $D = (\Sigma_g, \alpha, \beta)$ such that

- Σ_g is a closed oriented surface of genus $g \in \mathbb{N}$.
- $\alpha = (\alpha_1, \dots, \alpha_g)$ is a collection of g simple closed disjoint curves.
- $\beta = (\beta_1, \dots, \beta_g)$ is a collection of g closed immersed curves.
- The complement of α in Σ_g is connected.
- Every (self-)intersection of the curves is transverse.

We call *virtual Heegaard diagrams* the elements of D_{He}^v .

Remark : It is clear that a regular Heegaard diagram is also a virtual Heegaard diagram.

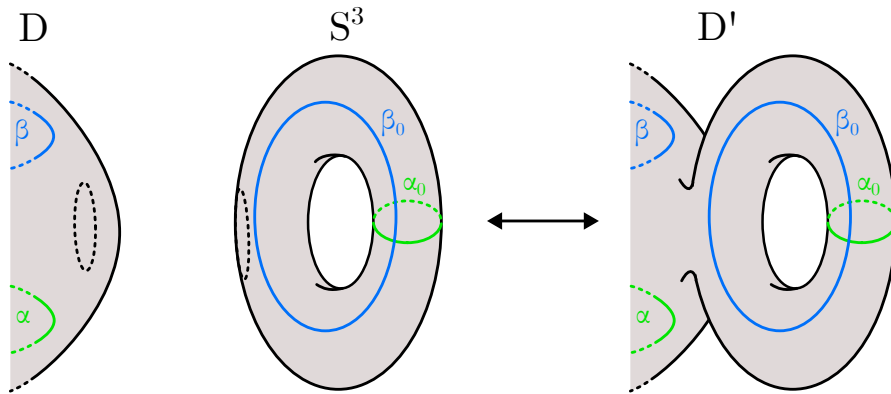


Figure 2: Stabilization on a diagram D or destabilization on a diagram D'

Definition 4.4. Let $D = (\Sigma_g, \alpha, \beta) \in D_{He}^v$ be a virtual Heegaard diagram. Let us consider the Heegaard diagram of genus 1 of the sphere S^3 , (T, α_0, β_0) (as represented in Figure 2). Let Σ'_g be a connected sum of Σ_g with the torus T along a disk disjoint from the sets of curves α, α_0, β and β_0 . Define $\alpha' = \alpha_0 \cup \alpha$ and $\beta' = \beta_0 \cup \beta$. We say that the virtual Heegaard diagram $D' = (\Sigma'_g, \alpha', \beta')$ is a *stabilization* of D .

Conversely, we say that D is a *destabilization* of D' .

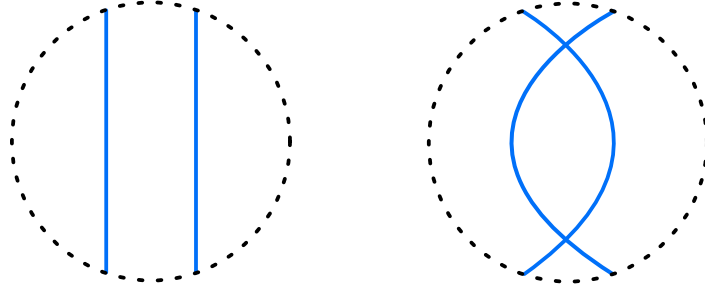


Figure 3: Diagrams differing by a R_{II} move (here, between β curves).

Definition 4.5. We say that two Heegaard diagrams are equivalent if we can link one to the other through a sequence of isotopies of the surface, handle-slides (of β curves or α curves between themselves), stabilizations and destabilizations, type 2 Reidemeister moves between β and α curves (also called R_{II} moves, see Figure 3) and orientation changes on α and β curves.

Theorem 4.6. *Two Heegaard diagrams representing the same manifold are equivalent.*

Remark : This Theorem (more details in [OS04, Theorem 2.9]) can be seen as a direct consequence or a Corollary of Reidemeister[Rei33]-Singer[Sin33]'s Theorem, for which proof can be found in [Lau14].

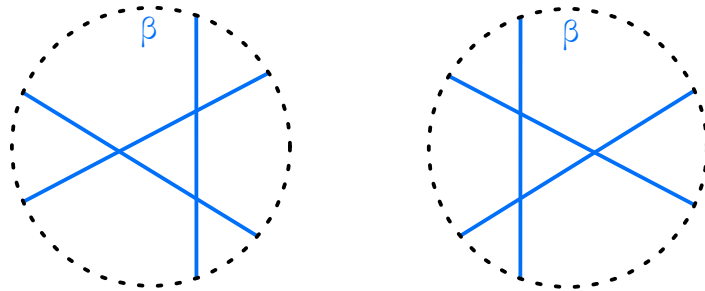


Figure 4: R_{III} move

On virtual Heegaard diagrams, we also consider the following moves :

- Handle slides of β curves over α curves,
- Type 3 Reidemeister moves between β curves (also called R_{III} moves (see Figure 4)),

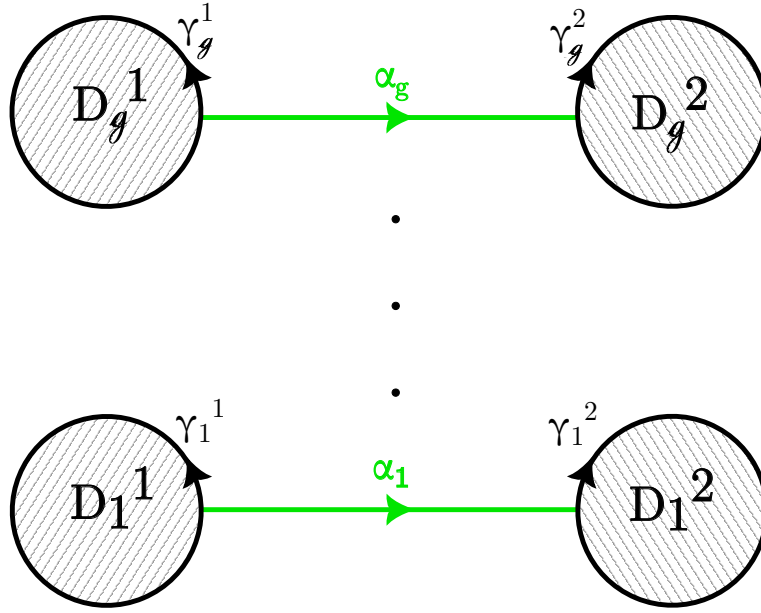


Figure 5: Genus g Heegaard diagram of \mathbb{S}^3

Remark : In the rest of this article, we use the diagram representations of [CC19] and described below.

Let g be a natural integer. We consider, in \mathbb{R}^2 , g pairs of disks $(D_i^1, D_i^2)_{1 \leq i \leq g} \subset \mathbb{R}^2$ of the same radius $< \frac{1}{3}$ and with centers $(1, i)$ and $(2, i)$, respectively. For each pair (D_i^1, D_i^2) , we consider α_i the minimum length segment connecting D_i^1 and D_i^2 , oriented from D_i^1 to D_i^2 . We see the boundaries of these disks as curves γ_i^1 and γ_i^2 , oriented such that their intersections with α_i verify $\alpha_i \cdot \gamma_i^1 = \alpha_i \cdot \gamma_i^2 = +1$ (see Figure 5).

We define the *geometric intersection matrix* of two families of g curves, α and γ , with transverse intersections, as $[\alpha \cap \gamma] := (\#\alpha_i \cap \gamma_j)_{i,j \in \{1, \dots, g\}}$.

Definition 4.7. We say that a Heegaard diagram $(\Sigma_g, \alpha, \gamma)$ of \mathbb{S}^3 is *standard* if $[\alpha \cap \gamma] = \text{Id}_g$ and if all intersections between α and γ are positive.

Let $(\Sigma_g, \alpha', \gamma')$ be a standard diagram of \mathbb{S}^3 , and let p_∞ be a point on the surface $\Sigma_g \setminus (\alpha' \cup \gamma')$. For all $i \in \{1, \dots, g\}$, let $V_i = \gamma'_i \times [-\varepsilon, \varepsilon]$ (with $\varepsilon > 0$) be a tubular neighborhood of γ'_i with its two boundaries denoted by $\gamma_i'^1 = \gamma'_i \times -\{\varepsilon\}$ and $\gamma_i'^2 = \gamma'_i \times \{\varepsilon\}$.

A *standard projection* is an orientation preserving diffeomorphism

$$\psi : \Sigma_g \setminus (\{p_\infty\} \cup \bigcup_{i \in \{1, \dots, g\}} \mathring{V}_i) \rightarrow \mathbb{R}^2 \setminus \bigcup_{i \in \{1, \dots, g\}, j \in \{1, 2\}} \mathring{D}_i^j$$

which sends the set of curves $\{\alpha'_i\}_{i \in \{1, \dots, g\}}$ over the previously described set of curves $\{\alpha\}_{i \in \{1, \dots, g\}}$. This induces that the boundaries $\{\gamma_i'^1\}_{i \in \{1, \dots, g\}}$ and $\{\gamma_i'^2\}_{i \in \{1, \dots, g\}}$ of $\Sigma_g \setminus (\{p_\infty\} \cup \bigcup_{i \in \{1, \dots, g\}} \mathring{V}_i)$ are mapped onto the boundaries $\{\gamma_i^1\}_{i \in \{1, \dots, g\}}$ and $\{\gamma_i^2\}_{i \in \{1, \dots, g\}}$ of

$\mathbb{R}^2 \setminus \bigcup_{i \in \{1, \dots, g\}, j \in \{1, 2\}} \mathring{D}_i^j$, respectively.

Let ϕ be the index permutation defined by $\psi(\alpha'_i) = \alpha_{\phi(i)}$ for all $i \in \{1, \dots, \mathbf{g}\}$. This permutation is also the one permuting the projections of the indices of γ'^1 and γ'^2 . Therefore, we find that $\psi((\alpha'_i, \gamma_i^1, \gamma_i^2)) = (\alpha_{\phi(i)}, \gamma_{\phi(i)}^1, \gamma_{\phi(i)}^2)$, for all $i \in \{1, \dots, \mathbf{g}\}$.

We can make the identification $\Sigma \setminus \gamma' \simeq \Sigma \setminus \overline{V}_i$. Through that identification, γ_i^1 and γ_i^2 represent the same curve γ'_i of $\Sigma_{\mathbf{g}}$. In the rest of this article, we will also use $\gamma_{\phi(i)}$ for such images obtained from a standard projection of curves γ'_i .

Remark : In [CC19] the notion of standard diagrams also appears, however, curves are non-oriented in that article.

Definition 4.8. Let $D = (\Sigma_{\mathbf{g}}, \alpha, \beta)$ be a virtual Heegaard diagram along with a fixed point $p_{\infty} \in \Sigma_{\mathbf{g}} \setminus (\alpha, \beta)$. Let us consider a family of curves $\gamma \subset \Sigma_{\mathbf{g}} \setminus \{p_{\infty}\}$ such that $(\Sigma_{\mathbf{g}}, \alpha, \gamma)$ is standard and that the intersections $\beta \cap \gamma$ are transverse. We then say that $(\Sigma_{\mathbf{g}}, \alpha, \beta, p_{\infty}, \gamma)$ is a *standardized diagram*.

Remark : For all virtual Heegaard diagrams $(\Sigma_{\mathbf{g}}, \alpha, \beta)$ and all fixed points $p_{\infty} \in \Sigma_{\mathbf{g}} \setminus (\alpha, \beta)$, there exists at least a family $\gamma \subset (\Sigma_{\mathbf{g}} \setminus \{p_{\infty}\})$ of \mathbf{g} simple disjoint closed curves such that $[\alpha \cap \gamma] = \text{Id}_{\mathbf{g}}$.

Indeed, the surface $\Sigma_{\mathbf{g}}$ with the α curves removed is diffeomorphic to an open disk with $2\mathbf{g} - 1$ holes. We can then establish on that disk a family $\gamma \subset \Sigma_{\mathbf{g}}$ of \mathbf{g} simple disjoint curves with connected complement, such that $[\alpha \cap \gamma] = \text{Id}_{\mathbf{g}}$.

Up to changes on the orientation of some curves of γ , we can deduce from this that there always exists a family of curves γ for which $(\Sigma_{\mathbf{g}}, \alpha, \gamma)$ is standard. Therefore, for all virtual Heegaard diagrams $(\Sigma_{\mathbf{g}}, \alpha, \beta)$, there exists at least one standardized virtual Heegaard diagram $(\Sigma_{\mathbf{g}}, \alpha, \beta, p_{\infty}, \gamma)$.

Definition 4.9. Let $(\Sigma_{\mathbf{g}}, \alpha, \beta, p_{\infty}, \gamma)$ be a standardized virtual Heegaard diagram. When we perform the connected sum between a curve β_j and the boundary of a tubular neighborhood of $\gamma_i \cup \alpha_i$, $i, j \in \{1, \dots, \mathbf{g}\}$, we say that we perform a G_{γ} move.

Examples :

The previously mentioned handle-slides of β over α , and G_{γ} moves can be represented on the plane \mathbb{R}^2 by standard projections, as pictured in Figures 6 and 7, respectively.

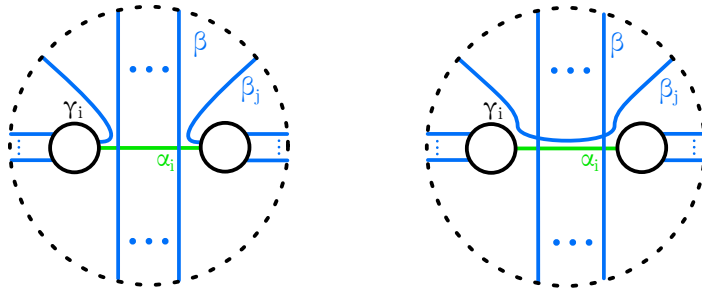


Figure 6: Handle-slide from a curve β_j over a curve α_i

Lemma 4.10. Let us consider two standard projections of the same diagram $(\Sigma_{\mathbf{g}}, \alpha, \gamma)$ along with a point $p_{\infty} \in \Sigma_{\mathbf{g}} \setminus (\alpha \cup \gamma)$. These projections differ by a diffeomorphism of $\mathbb{R}^2 \setminus (\bigcup_{i \in \{1, \dots, \mathbf{g}\}} D_i^1 \cup D_i^2)$ composed of isotopies fixing $\alpha \cup \gamma$, of Dehn twists along the boundary of disks, each containing a single pair $(\gamma_i, \alpha_i)_{i \in \{1, \dots, \mathbf{g}\}}$, and of diffeomorphisms representing a generator of the braid group on \mathbf{g} strands.

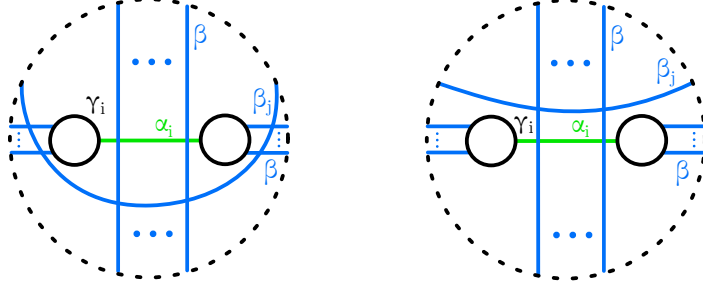


Figure 7: Two diagrams differing by a G_γ move from the curve β_j over $\gamma_i \cup \alpha_i$

Proof. Let us consider two standard projections of the same diagram $D = (\Sigma_g, \alpha, \gamma)$ along with a point $p_\infty \in \Sigma_g \setminus (\alpha \cup \gamma)$. The images of D by these projections differ by a diffeomorphism of \mathbb{R}^2 fixing the set of pairs $\{(\gamma_i, \alpha_i)\}_{i \in \{1, \dots, g\}}$. Each pair $(\gamma_i, \alpha_i)_{i \in \{1, \dots, g\}}$ lies within a disk, as each $\gamma_i \cup \alpha_i$ admits a neighborhood isomorphic to a disk in \mathbb{R}^2 . Therefore, we can see the classes of these diffeomorphisms (modulo isotopies fixing $\alpha \cup \gamma$) as the set of braids on g strands in the plane, with framing on each strand.

Artin's theorem gives a family of generators $(\omega_i)_{i \in \{1, \dots, g-1\}}$ for these diffeomorphisms.

Theorem 4.11 (Artin [Art25]). *The braid group on n strands in the plane admits a presentation with generators $\omega_1, \dots, \omega_{n-1}$ and defining relations*

- $\omega_i \omega_j = \omega_j \omega_i$ if $|i - j| \geq 2$, $i, j \in \{1, \dots, n - 1\}$,
- $\omega_i \omega_{i+1} \omega_i = \omega_{i+1} \omega_i \omega_{i+1}$ for all $i \in \{1, \dots, n - 1\}$.

More details in [Bir74, Th. 1.8].

Now, it remains to observe the difference between two diffeomorphisms for which their associated braids have differing framings. Since the boundaries of the disks are fixed, the change induced on the framing by any considered diffeomorphism will be an element of \mathbb{Z}^g . A difference between two projections of one positive turn on the framing over one of the fixed disks amounts to performing, in the diagram, a Dehn twist around that disk. Therefore, we find the desired result. \square

We introduce virtual Heegaard diagrams because, unlike regular Heegaard diagrams, every virtual Heegaard diagram can be associated to a diagram whose family of β curves can be entirely projected onto the plane $\mathbb{R}^2 \setminus (\bigcup_{i \in \{1, \dots, g\}} D_i^1 \cup D_i^2)$. We will call *flat* such a diagram.

Definition 4.12 (Flat diagrams). Let us consider a diagram $D = (\Sigma_g, \alpha, \beta) \in D_{He}^v$ and a fixed point $p_\infty \in \Sigma_g \setminus (\alpha \cup \beta)$. We say that (D, p_∞) is *flat* with regard to a set of curves $\gamma \subset \Sigma_g \setminus p_\infty$ (or γ -flat) if the sets β and γ never intersect each other.

Let us consider two virtual Heegaard diagrams $D = (\Sigma_g, \alpha, \beta) \in D_{He}^v$ and $D' = (\Sigma_g, \alpha, \beta') \in D_{He}^v$, a fixed point $p_\infty \in \Sigma_g \setminus (\alpha \cup \beta \cup \beta')$ and a set of curves $\gamma \subset (\Sigma_g \setminus \{p_\infty\})$ such that the $\beta \cap \gamma$ intersections are transverse. We say that (D', p_∞) is a *flattening* of (D, p_∞) with regards to γ (or γ -flattening of (D, p_∞)) if β' and γ never intersect each other, and if D' is linked to D through a sequence of handle-slides of β curves over α , moves R_{II} between β curves or between β and α curves, moves R_{III} between β curves and isotopies of the pointed surface (Σ_g, p_∞) with each move operated within an open set not containing p_∞ . We will sometimes simply say that D' is a γ -flattening of D .

Remark : Two flattenings of the same virtual Heegaard diagram, with the same point p_∞ and the same family of curves γ will always be linked by a sequence of moves R_{II} between β curves or between β and α curves, moves R_{III} between β curves, isotopies of the pointed surface (Σ_g, p_∞) and moves G_γ (see Figure 7) with each move operated within an open set not containing p_∞ .

Proposition 4.13. *Let us consider a virtual Heegaard diagram $D = (\Sigma_g, \alpha, \beta) \in D_{He}^v$, and a fixed point $p_\infty \in \Sigma_g \setminus (\alpha \cup \beta)$. Let $\gamma \subset (\Sigma_g \setminus \{p_\infty\})$ be a family of g simple disjoint closed curves such that $[\alpha \cap \gamma] = \text{Id}_g$, and that all intersections $\beta \cap \gamma$ are transverse. Then, there exists a γ -flattening of D .*

Remark : We note that $[\alpha \cap \gamma] = \text{Id}_g$ induces that α and γ each have connected complement.

Proof. Let us consider a virtual Heegaard diagram $D = (\Sigma_g, \alpha, \beta) \in D_{He}^v$, and a fixed point $p_\infty \in \Sigma_g \setminus (\alpha \cup \beta)$. Let $\gamma \subset (\Sigma_g \setminus \{p_\infty\})$ be a family of g simple disjoint closed curves such that $[\alpha \cap \gamma] = (\delta_{ij})_{i,j \in \{1, \dots, g\}}$, and that all intersections $\beta \cap \gamma$ are transverse. For all $i \in \{1, \dots, g\}$, we denote by $p_i \in \gamma_i$ the intersection point defined by $\alpha_i \cup \gamma_i = \{p_i\}$.

Let us assume that the set $\beta \cap \gamma$ is non-empty (else the diagram is already flat). Then, there exists a crossing $c \in \beta \cap \gamma$ on a curve $\gamma_i \in \gamma$ such that the segment of γ_i between p_i and c does not intersect β . We denote by $\beta_j \in \beta$ the β curve on which c is placed.

By an isotopy of the surface $\Sigma_g \setminus (p_\infty \cup \alpha)$, we can slide the crossing c along the previously mentioned segment of γ_i until it is sufficiently close to p_i . We can then perform a handle-slide of β_j over α_i . Since an open segment of β_j centered at c is now parallel to an open segment of α_i centered at p_i , the crossing is erased by the handle-slide and no new crossing appeared because, by our initial hypothesis, α_i intersects γ only at p_i .

By induction on the number of crossings between β and γ , we can recover a γ -flattening of (D, p_∞) . □

Remark : Since the α curves are all disjoint and $\gamma_i \cap \alpha = \{p_i\}$, we notice that the process used in the proof does not induce any additional crossing between β and α .

Definition 4.14. A standardized virtual Heegaard diagram $(\Sigma_g, \alpha, \beta, p_\infty, \gamma)$ is called *standardized flat* if $((\Sigma_g, \alpha, \beta), p_\infty)$ is flat with regards to γ .

It results from Proposition 4.13 and the Remark following Definition 4.8 that, for any virtual Heegaard diagram $(\Sigma_g, \alpha, \beta)$ and any point $p_\infty \in \Sigma_g \setminus (\alpha \cup \beta)$, there exists a family of curves γ and a family of curves β' such that $((\Sigma_g, \alpha, \beta'), p_\infty)$ is a γ -flattening of $((\Sigma_g, \alpha, \beta), p_\infty)$. Therefore, there always exists at least one standardized flat virtual Heegaard diagram $(\Sigma_g, \alpha, \beta', p_\infty, \gamma)$ associated to $(\Sigma_g, \alpha, \beta)$.

4.2 The map F'' over virtual Heegaard diagrams

Let $D = (\Sigma_g, \alpha, \beta, p_\infty, \gamma)$ be a standardized flat virtual Heegaard diagram. Any standard projection ψ of $((\Sigma_g, \alpha, \beta), p_\infty)$ produces an image $(\alpha', \beta') = \psi(\alpha, \beta)$ in the plane with $2g$ disks removed. We call \mathfrak{D} the set of all such images of standard projection.

Definition 4.15. We define the map $F''_H : \mathfrak{D} \rightarrow \mathbb{k}$ by the following algorithm.

Let us consider $(\alpha', \beta') \in \mathfrak{D}$. By definition of \mathfrak{D} , (α', β') is the image, by a standard projection, of a standardized flat virtual Heegaard diagram $D = (\Sigma_g, \alpha, \beta, p_\infty, \gamma)$. In the rest of this article, we will identify α' and β' with their preimages under ψ , we will thus denote them α and β respectively.

- We place a unique base point p_i on each component β_i of β .
- For every component $\alpha_k \in \alpha$ such that $\alpha_k \cap \beta \neq \emptyset$, we apply the action of Λ to all crossings with β . In other words, let n be the cardinal of $\alpha_k \cap \beta$, and $\Lambda_{(j)}$ be the j -nth factor of the coproduct $\Delta^{(n)}(\Lambda)$ (as indicated by (1)). We locally add to the j -nth crossing of α_k , on the curve β_i of β involved in the crossing, the bead

$$S^{d_j}(\Lambda_{(j)}) \quad \text{where } d_j = \begin{cases} 1 & \text{if } (\vec{\alpha}_k, \vec{\beta}_i) \text{ has negative orientation at the crossing,} \\ 0 & \text{else (see Figure 8).} \end{cases}$$

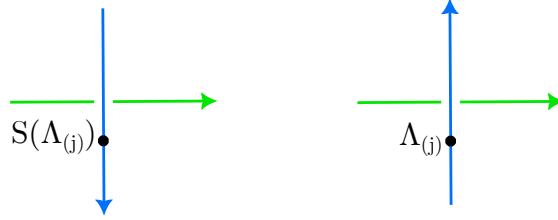


Figure 8: Beads placement at the crossing between curves α_k and β_j

We then work with sums of diagrams, where only the bead's values change (see in the example Figure 10). Accordingly, "the bead x " refers to the corresponding x bead on every diagram in the summation.

- We then add on each "cap" and "cup" of β the beads g as indicated in Figure 9. (We note that these are the same bead placements as in 1.)



Figure 9: Placement of g beads on β

- For each component $\beta_i \in \beta$, we follow its orientation starting from the base point, and multiply every bead accordingly (the multiplication is performed from the left). This gives us a total bead b_i . If there is no bead on β_i , we consider $b_i = 1_H$.
- The image of F'' is given by

$$F''_H(\psi(\alpha, \beta)) := \epsilon(\Lambda)^v \prod_{i=1}^g \mu(b_i),$$

where $v \in \mathbb{N}$ is the number of components $\alpha_k \in \alpha$ such that $\alpha_k \cap \beta = \emptyset$.

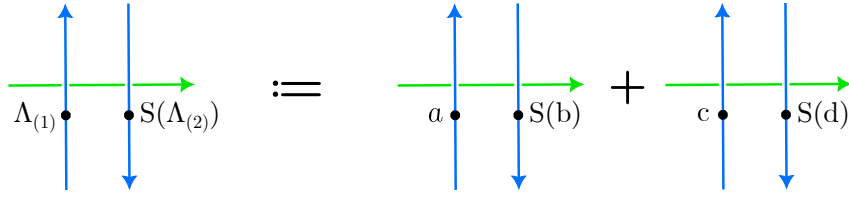


Figure 10: Notation example when $\Delta^{(2)}(\Lambda) = a \otimes b + c \otimes d$

The map F'' is well defined because, by property of the symmetrized integral, for all $x, y \in H$ we have $\mu(xy) = \mu(yx)$. Hence, F'' is independent of the choice of base point placement.

Proposition 4.16. *Let $(\Sigma_g, \alpha, \beta, p_\infty, \gamma)$ be a standardized flat virtual Heegaard diagram. Two elements of \mathfrak{D} recovered from $(\Sigma_g, \alpha, \beta, p_\infty, \gamma)$ will have the same image by F'' . Therefore, we can define*

$$F''(\Sigma_g, \alpha, \beta, p_\infty, \gamma) = F''(\psi(\alpha, \beta))$$

where ψ is any standard projection of $((\Sigma_g, \alpha, \gamma), p_\infty)$.

Proof. Let $D = (\Sigma_g, \alpha, \beta, p_\infty, \gamma)$ be a standardized flat virtual Heegaard diagram.

We have previously seen in Lemma 4.10 that two projections differ by a diffeomorphism composed of isotopies (fixing α and γ curves), of Dehn twists around disks containing each a pair $(\gamma_i, \alpha_i)_{i \in \{1, \dots, g\}}$, and of diffeomorphisms representing the generators of the braid group on g strands. Thus, we want to show that F''_H is invariant by these elements.

Let us consider the images of two standard projections of the same diagram, and assume that these projections differ only by an isotopy of the plane fixing the α and γ curves. Such an isotopy does not change the crossings between α and β on the images of the diagram. If it modifies the extrema of the β curves between the images of both projections, the change induced will always be the appearance (or vanishing) of a pair of a consecutive minimum and maximum with the same orientations. Hence, depending of the orientation of the curves affected by the isotopy, either no bead appears, or a bead colored by g and a bead colored by g^{-1} will appear consecutively. Therefore, F''_H is invariant by isotopies of the plane fixing the α and γ curves.

The computational algorithm of F'' allows us to note the following point ; If two elements of \mathfrak{D} have the same crossings $\alpha \cap \beta$ (orders and orientations over the curves α and β) and the same local minima and maxima over the β curves (positions on β relative to the crossings $\alpha \cap \beta$ and orientations included), then these two diagrams will have the same image by F''_H . In the case of images by two standard projections of the same diagram, they directly admit the same crossings $\alpha \cap \beta$, therefore, it is enough to focus on the minima and maxima of β curves.

We can also deduce, in a more general setting, that two elements of \mathfrak{D} differing by the image of an R_{II} move (see Figure 3), an R_{III} move (see Figure 4) or a G_γ move (see Figure 7) on $\Sigma \setminus (\alpha \cup \gamma \cup p_\infty)$ will have the same image by F''_H , for these moves do not influence the crossings between β and α , neither do they influence the extrema of β . In the rest of this article, we sometimes use these moves to simplify diagrams without changing their image by F''_H .

Let us consider two projections of the same diagram that differ only by a Dehn twist around a fixed disk containing a pair (γ_i, α_i) (and not containing any other pair

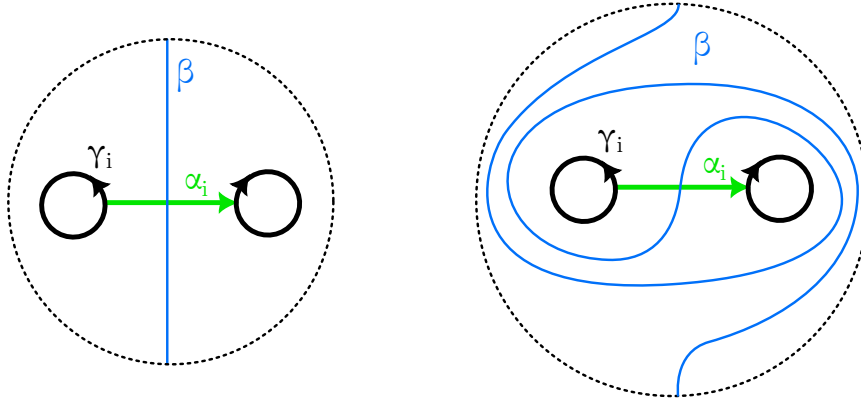


Figure 11: Two projections of the same diagram differing by a Dehn twist

$(\gamma_j, \alpha_j), j \neq i$). We can see this difference in Figure 11 (where the vertical segment β represents multiple parallel strands of β). For each strand $\beta_k \in \beta$ intersecting α_i in the right figure (Figure 11) we collect a bead b'_i on the represented segment. If the segment is oriented upward, we see a bead g^{-1} appear before the crossing $\alpha_i \cap \beta_k$ and a bead g after the same crossing. The same situation arises if the segment is oriented downward. Therefore, $b'_i = gS^{d_k}(\Lambda_{(i_k)})g^{-1} = S^{d_k+2}(\Lambda_{(i_k)})$, with $d_k = 0$ or 1 depending on the sign on the crossing $\alpha_i \cap \beta_k$, and i_k is the index indicating the order in which α_i crosses the strands of β . However, we recall that $\bigotimes_j S^2(\Lambda_{(j)}) = \bigotimes_j (S^2(\Lambda))_{(j)} = \bigotimes_j \Lambda_{(j)}$ because H is unimodular. Hence, on each segment we recover the bead collected on the corresponding segment in the left figure (Figure 11). Thus, both projections will give the same image by F'' .

The generators $\omega_1, \dots, \omega_{g-1}$ of the braid group on g strands, mentioned in Theorem 4.11, can be represented by the following diffeomorphisms (see Figure 12). Let W_1, \dots, W_g be closed connected neighborhoods in \mathbb{R}^2 of the pairs $(\alpha_1 \cup \gamma_1), \dots, (\alpha_g \cup \gamma_g)$, respectively. For all $i, j \in \{1, \dots, g\}$, we consider V_i a ring ($\simeq \mathbb{S}^1 \times]-\epsilon, \epsilon[$ with $\epsilon > 0$) such that $(W_i \cup W_{i+1}) \subset V_i$ and $V_i \cap W_j = \emptyset$ for all $j \notin \{i, i+1\}$. Each diffeomorphism representing a generator ω_i is isotopic to the identity on $\text{Diff}(\mathbb{R}^2)$ by an isotopy of \mathbb{R}^2 . This isotopy is the identity on $\mathbb{R}^2 \setminus V_i$ and rotates W_i and W_{i+1} inside V_i by an angle $t \in [0, \pi]$, while keeping the α curves horizontal. (Each diffeomorphism is isotopic to the identity inside the diffeomorphisms of \mathbb{R}^2 , but not inside those of $\mathbb{R}^2 \setminus \bigcup_{i \in \{1, \dots, g\}, j \in \{1, 2\}} D_i^j$.)

The action of a generator ω_i on a standard projection translates graphically as shown in Figure 12 (where the vertical segment β represents multiple parallel strands of β). If a strand of β (other than those represented in Figure 12) intersects the neighborhood V_i , we can make V_i "sufficiently thin" for that strand to simply cut across V_i . It will be subject to an isotopy on V_i , which, as seen, previously, does not influence its image by F''_H .

If a strand of β_k intersecting α_i or α_{i+1} in Figure 12 is oriented upward, no bead will appear on its extrema. If the strand of β intersecting α_i (respectively α_{i+1}) is oriented downward, before its intersection with α_i (resp. after its intersection with α_{i+1}) a bead g^{-1} , and then a bead g , will appear consecutively on the right figure (Figure 12). During the bead multiplication, it will result in a trivial bead 1_H . Hence, both projections will give the same image by F''_H .

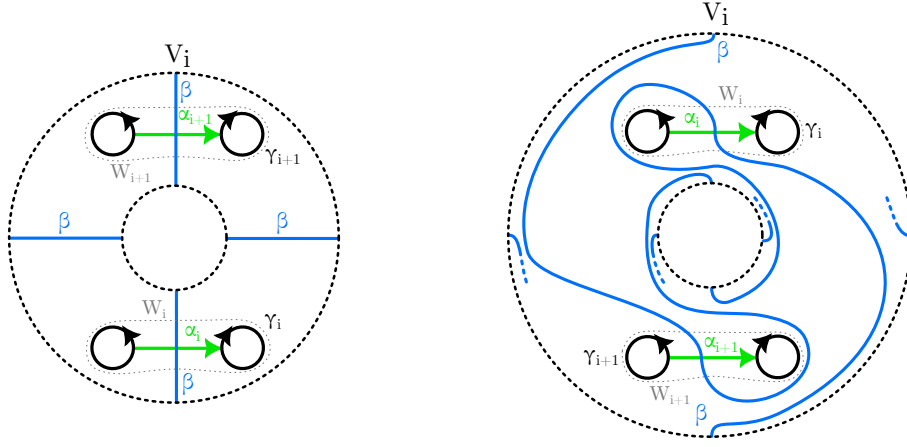


Figure 12: effect of ω_i on a diagram's projection (Σ, α, β) (initial diagram on the left, effect of ω_i on the right)

Therefore, F''_H is independent of the choice of the standard projection used to send the diagram onto \mathbb{R}^2 with $2g$ disks removed. \square

Proposition 4.17. *The map F'' is invariant under orientation reversal of a β curve as well as invariant under orientation reversal of an α curve and its associated γ curve.*

Proof. Let $D = (\Sigma_g, \alpha, \beta, p_\infty, \gamma)$ be a flat virtual Heegaard diagram. Let us consider a virtual Heegaard diagram $(\Sigma_g, \alpha, \bar{\beta})$ differing from $(\Sigma_g, \alpha, \beta)$ only over the orientation of a curve β_i (we will denote $\beta_i \in \bar{\beta}$ the curve β_i with reverse orientation). The diagram $\bar{D} = (\Sigma_g, \alpha, \bar{\beta}, p_\infty, \gamma)$ obtained this way is also a flat virtual Heegaard diagram. We project D and \bar{D} onto the plane with the same standard projection ψ .

We start by decomposing β_i into segments over which we will observe the effects of the orientation reversal. We divide $\beta_i \in \beta$ into two types of segments,

1. a first type being segments containing only a local maximum, then a number $n \in \mathbb{N}$ of crossings between β_i and α (potentially with crossing between β_i and β in between), and then a local minimum,
2. a second type being segments forming the complement over β_i of first-type segments.

During the computation of F'' , the symmetrized integral's property $\mu(z, y) = \mu(y, z)$ allows us to assume that the base points of β_i and $\bar{\beta}_i$ are at the end of a segment. Therefore, during the bead collection, we can consider one bead per segment. On a segment, we denote by $x \in H$ the collected bead on β_i and by $\bar{x} \in H$ the collected bead on $\bar{\beta}_i$.

By definition, β_i is oriented upward on second-type segments, hence, only beads originating from positive crossings of β_i with α will appear on these segments. Thus, the definition of beads on crossings, together with the relation $S(x)S(y) = S(yx)$, allows us to see that $\bar{x} = S(x)$.

Over first-type segments, we notice that every crossing of β_i with α will be negative. The relation $\bar{x} = S(x)$ does not directly appear but can be obtained by properties of the antipode and pivot.

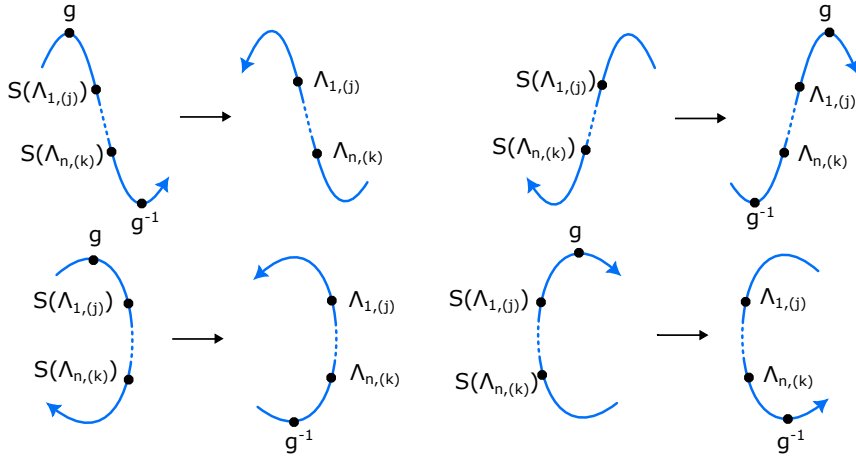


Figure 13: Orientation reversal on first-type segments (with n beads originating from crossings between β_i and α).

For example, in the case represented in the upper left side of Figure 13, we notice that $x = g^{-1}S(\Lambda_{n,(k)}) \cdots S(\Lambda_{1,(j)})g$ and $\bar{x} = \Lambda_{1,(j)} \cdots \Lambda_{n,(k)}$ where each $\Lambda_{p,(q)}$, $p, q \in \mathbb{N}$, originates from a $\Lambda_p = \Lambda$ by coproduct, as indicated in notation (1). However,

$$S(g^{-1}S(\Lambda_{n,(k)}) \cdots S(\Lambda_{1,(j)})g) = g^{-1}S^2(\Lambda_{1,(j)}) \cdots S^2(\Lambda_{n,(k)})g = \Lambda_{1,(j)} \cdots \Lambda_{n,(k)}.$$

We then recover the relation $\bar{x} = S(x)$ for that case. All other cases are represented in Figure 13 and result in the same relation through analogous reasoning. Therefore, every bead originating from a first type segment verifies the relation $\bar{x} = S(x)$.

Let b_i and \bar{b}_i be the total beads of β_i and $\bar{\beta}_i$, respectively. Since $\mu \circ S = \mu$, we deduce that $\mu(b_i) = \mu(\bar{b}_i)$, which allows us to conclude the invariance of F'' under reversal of a β curve's orientation.

Let us consider this time a diagram \bar{D} differing from D only over the orientation of a curve α_i (we will denote $\bar{\alpha}_i \in \bar{\alpha}$ the curve α_i with reverse orientation). The family of curves $\bar{\gamma}$ associated to \bar{D} will be identical to γ except on the curve γ_i where it will have reverse orientation (we will denote $\bar{\gamma}_i \in \bar{\gamma}$ the curve γ_i with reverse orientation). We can then consider standard projections such that the images of D and \bar{D} differ only on an open disk such as represented in Figure 14.

Here, we will use the property $\Delta^{(n)}(S(x)) = S(x_{(n)}) \otimes \cdots \otimes S(x_{(1)})$ from the coproduct and antipode. If a strand from β is oriented upward, then no bead $g^{\pm 1}$ appears after the change. However the bead $\Lambda_{(i)}$ at the crossing becomes $S(\Lambda_{(l-i+1)}) = S(\Lambda_{(i)})$, with $l \in \mathbb{N}$ the number of crossings of α_i with β . If a strand of β is oriented downward, then a bead g and a bead g^{-1} appear before and after the crossing, respectively. Furthermore, the bead $S(\Lambda_{(i)})$ at the crossing becomes $\Lambda_{(l-i+1)} = S^{-1}(S(\Lambda_{(i)}))$. The product of these three beads is $g\Lambda_{(l-i+1)}g^{-1} = S(S(\Lambda_{(i)}))$ as g is a pivot of H . Since H is unimodular we have $S(\Lambda) = \Lambda$, which induces that, for all $n \in \mathbb{N}$, $\Lambda_{(1)} \otimes \Lambda_{(2)} \otimes \cdots \otimes \Lambda_{(n)} = S(\Lambda_{(n)}) \otimes \cdots \otimes S(\Lambda_{(2)}) \otimes S(\Lambda_{(1)})$. Therefore, both projections will give the same image by F'' , thus F''_H is invariant under orientation reversal of an α curve and its associated γ curve. \square

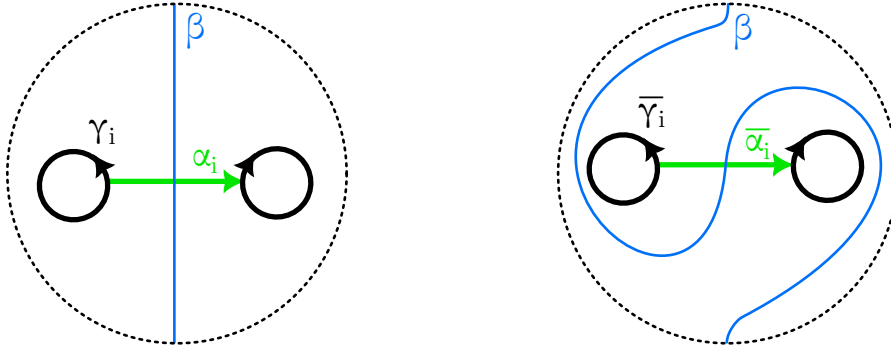


Figure 14: Impact on the image in the plane of an orientation reversal on a curve α_i (here β represent multiple parallel β curves)

The map F_H'' can be extended to all virtual Heegaard diagrams as follows.

Proposition 4.18. *Let $D = (\Sigma_g, \alpha, \beta, p_\infty, \gamma)$ be a standardized virtual Heegaard diagram. We define the image of D under F_H'' as follows*

$$F_H''(D) := F_H''(\Sigma_g, \alpha, \beta', \gamma, p_\infty)$$

where $(\Sigma_g, \alpha, \beta')$ is a γ -flattening of $(\Sigma_g, \alpha, \beta)$. The image $F_H''(D)$ is independent of the choice of γ -flattening.

Proof. Let $D = (\Sigma_g, \alpha, \beta, p_\infty, \gamma)$ be a standardized virtual Heegaard diagram.

For the image of $F_H''(D)$ to be well defined, it is necessary that F_H'' has the same image for any γ -flattening of $(\Sigma_g, \alpha, \beta)$. We have mentioned that, by definition, two (γ -)flattening of the same virtual Heegaard diagram are linked by a sequence of R_{II} moves between β curves or between β and α curves, R_{III} moves between β curves, isotopies of the pointed surface (Σ_g, p_∞) , and G_γ moves, with each move operated within an open set not containing p_∞ . Hence, we want to prove that F_H'' is invariant by these operations. We also recall (seen in the proof of Proposition 4.16) that only operations which alter the crossings between α and β curves, or the β curves' extrema, can change the image under F_H'' .

Two standardized virtual Heegaard diagrams differing by an isotopy of the pointed surface (Σ_g, p_∞) admit two standard projections differing by an isotopy of the plane leaving $\alpha \cup \gamma$ fixed. However, we have also shown (in proof of Proposition 4.16) that F_H'' is invariant by isotopies of the plane leaving $\alpha \cup \gamma$ fixed, by G_γ moves, and by R_{III} and R_{II} moves between β curves in $\Sigma \setminus (\alpha \cup \gamma \cup p_\infty)$. Therefore, two flattenings differing by these moves will have the same image.

We now have only to show that F_H'' is invariant by R_{II} moves between β and α curves.

Let $D = (\Sigma_g, \alpha, \beta, p_\infty, \gamma)$ and $D' = (\Sigma_g, \alpha, \beta', p_\infty, \gamma)$ be two standardized virtual Heegaard diagrams, identical except on an open set V where they differ by an R_{II} move as shown in Figure 15.

Let us consider a component $\beta_i \in \beta$, $i \in \{1, \dots, g\}$, we denote by b_i the total bead recovered on the left diagram (Figure 15) and b'_i the total bead recovered on the right diagram. If the curve β_i is oriented from right to left, then no bead g appears on the diagrams. The curve $\alpha_k \in \alpha$, $k \in \{1, \dots, g\}$, involved will always be oriented from left

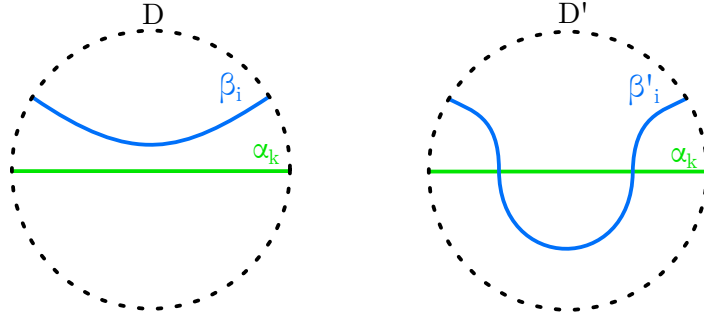


Figure 15: R_{II} move between an α curve and a β curve

to right, by definition of a standard projection. We denote by $m \in \mathbb{N}$ the integer such that the R_{II} move between α_k and β_i is performed just after $m - 1$ crossings. Hence, let $A_{i,m}$ and $B_{i,m}$ be the products of collected beads on β_i before and after the considered open set, respectively, we have, for the left diagram, $b_i = B_{i,m}A_{i,m}$ and, for the right diagram, $b'_i = B_{i,m}(\Lambda_{k,(m)})_{(1)}S((\Lambda_{k,(m)})_{(2)})A_{i,m}$.

By definition of the antipode, $(\Lambda_{k,(m)})_{(1)}S((\Lambda_{k,(m)})_{(2)}) = \epsilon(\Lambda_{k,(m)})$ and, by property of the coproduct, for all $n \geq 1$ and all $x \in H$, we have $x_{(1)} \otimes \cdots \otimes x_{(m-1)} \otimes \epsilon(x_{(m)}) \otimes x_{(m+1)} \otimes \cdots \otimes x_{(n)} = \Delta^{(n-1)}(x)$. Let $l \geq 2$ be the number of crossings between β and α_k . If $l > 2$, the previous equality allows us to recover the action of Λ_k on the remaining $l - 2$ crossings with α_k . If $l = 2$, the equality produces the term $\epsilon(\Lambda_k) = \epsilon(\Lambda)$ which is the term added to the final product when a curve α_k does not intersect β . Thus we find the same images by F''_H for the right diagram and for the left diagram (in Figure 15).

If the curve β_i is oriented from left to right, then a bead g^{-1} appears on its local minimum. In the same way as before, we get for the left diagram the total bead $b_i = B_{i,m}g^{-1}A_{i,m}$ and for the right diagram the total bead $b'_i = B_{i,m}(\Lambda_{k,(m)})_{(2)}g^{-1}S((\Lambda_{k,(m)})_{(1)})A_{i,m}$. By definition of the antipode S and pivot g , we can simplify the bead b'_i .

$$\begin{aligned} B_{i,m}(\Lambda_{k,(m)})_{(2)}g^{-1}S((\Lambda_{k,(m)})_{(1)})A_{i,m} &= B_{i,m}g^{-1}S^2((\Lambda_{k,(m)})_{(2)})S((\Lambda_{k,(m)})_{(1)})A_{i,m} \\ &= B_{i,m}g^{-1}S((\Lambda_{k,(m)})_{(1)})S((\Lambda_{k,(m+1)})_{(2)})A_{i,m} \\ &= B_{i,m}g^{-1}\epsilon(\Lambda_{k,(m)})A_{i,m}. \end{aligned}$$

Therefore, the same equalities and reasoning as before apply, and we recover the same final image under F''_H for both diagrams.

Analogous reasoning also applies for an R_{II} move where the β curve is placed under the α curve. Hence, we can conclude our proof. \square

Remark : It is strongly suspected, but remains unproven, that the map F''_H on standardized virtual Heegaard diagrams is also independent of the choice of the family of curves γ .

4.3 The chromatic spherical invariant \mathcal{K}

In this part, we will prove the link between the 3-manifolds invariant $\mathcal{K}_{H\text{-mod}}$ defined in [CGPMT20] (with $H\text{-mod}$ the category of finite-dimensional pivotal H -modules) and

the map F_H'' previously defined. Before proving this link, we start by defining $\mathcal{K}_{H\text{-mod}}$ using results from [CGPMT20].

We consider the left H -module H defined by the action $L : H \rightarrow \text{End}_{\mathbb{k}}(H)$ giving $L_h(x) = hx$ for all $h, x \in H$. In particular, H seen as such is a projective generator of $H\text{-mod}$. We denote by Proj_H the ideal of projective modules from the pivotal category $H\text{-mod}$.

The definition of $\mathcal{K}_{H\text{-mod}}$ relies on the category of $H\text{-mod}$ -colored ribbon graphs over multi-handlebodies as defined below (see [Tur10]). We call *multi-handlebodies* a disjoint union of a finite number of 3-dimensional oriented handlebodies.

A $H\text{-mod}$ -colored ribbon graph over a multi-handlebody \mathfrak{C} is a finite graph embedded in $\partial\mathfrak{C}$ with each edge colored with an object of $H\text{-mod}$ and each vertex thickened in $\partial\mathfrak{C}$ into a coupon colored by a morphism of $H\text{-mod}$. Every coupon has a top and a bottom. Since the graphs are considered on an oriented surface, they possess a natural framing with its ribbon structure given by thickening the graph in the surface $\partial\mathfrak{C}$ (see [Tur10] for more details on ribbon graphs). We say that a graph is Proj_H -colored if all its colors are elements of Proj_H .

Definition 4.19. A *bichrome graph* on a handlebody is a graph on the boundary of a handlebody that is partitioned into two disjoint subgraphs, one red, the other blue, such that the blue subgraph is $H\text{-mod}$ -colored and that the red subgraph is a disjoint union of unoriented simple closed curves.

For the computation of $\mathcal{K}_{H\text{-mod}}$ which follows, we will consider Proj_H -colored graphs and we can even restrict ourselves to graphs where all edges are colored by H .

On bichrome graphs, it is possible to apply a "red to blue" or "chromatic" modification (see Figure 16). It is a local modification allowing a curve from the red subgraph to pass into the blue subgraph thanks to a category morphism, called chromatic morphism (more details in [CGPMT20]).

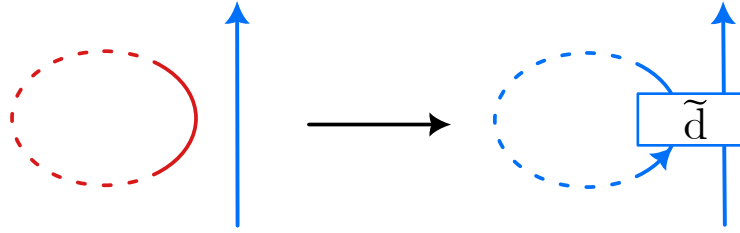


Figure 16: Chromatic modification with the chromatic morphism \tilde{d} .

By Theorem [CGPMT20, 2.5], since H is a spherical Hopf algebra, there exists a non-degenerate modified trace τ (defined in [GPMV13]) over the ideal Proj_H , and a chromatic morphism $\tilde{d} : H \otimes H \rightarrow H \otimes H$. This trace is unique (up to a scalar) and determined by $\tau_H(f) = \mu(f(1))$ for all $f \in \text{End}_H(H)$ (see [BBG21, Th.1]). We define a chromatic morphism $\tilde{d} : H \otimes H \rightarrow H \otimes H$ (introduced in [CGPMT20]) by

$$\tilde{d}(x \otimes y) = \lambda(S(y_{(1)})gx)y_{(2)} \otimes y_{(3)} \quad \text{for } x \otimes y \in H \otimes H.$$

Let \mathcal{H}_B be the set of pairs (\mathfrak{C}, Γ) with \mathfrak{C} a handlebody and Γ a bichrome graph on \mathfrak{C} with a non-empty blue subgraph. Let F be the pivotal functor associated with Penrose graphical calculus (more details in [Tur10]). [CGPMT20, Theorem 2.1] applied

to the pivotal category $\mathcal{H}\text{-mod}$ allows us to define F' , an invariant on \mathcal{H}_B , through the following theorem.

Theorem 4.20. *There exists a unique map $F' : \mathcal{H}_B \rightarrow \mathbb{k}$ satisfying the following four conditions.*

1. *The element $F'(\mathfrak{C}, \Gamma) \in \mathbb{k}$ depends only on $(\mathfrak{C}, \Gamma) \in \mathcal{H}_B$, up to orientation preserving diffeomorphisms.*
2. *For all Proj_H -colored ribbon graphs (B^3, Γ) on the 3-ball, we have $F'(B^3, \Gamma) = \tau(F(T))$ where T is a bichrome graph representing an element of $\text{End}_{\mathbb{k}}(P)$, with $P \in \text{Proj}_H$, admitting Γ as its braid closure.*
3. *For all $(\mathfrak{C}_1, \Gamma_1), (\mathfrak{C}_2, \Gamma_2) \in \mathcal{H}_B$, we have*

$$F'(\mathfrak{C}_1 \sqcup \mathfrak{C}_2, \Gamma_1 \sqcup \Gamma_2) = F'(\mathfrak{C}_1, \Gamma_1)F'(\mathfrak{C}_2, \Gamma_2).$$

4. *Let D be a 2-disk disjoint from the red subgraph and intersecting at least one blue edge. If we cut $(\mathfrak{C}, \Gamma) \in \mathcal{H}_{\text{Proj}_H}$ along D (as described below), we have $F'(\text{cut}_D(\mathfrak{C}), \text{cut}_D(\Gamma)) = F'(\mathfrak{C}, \Gamma)$.*
5. *If $\Gamma, \Gamma' \in \mathcal{H}_B$ are linked by a chromatic modification, then $F'(\Gamma) = F'(\Gamma')$.*

We now define what *cutting* a multi-handlebody and a bichrome graph means for us. Cutting an element $(\mathfrak{C}, \Gamma) \in \mathcal{H}_B$ along a disk D (with $\partial D \subset \partial \mathfrak{C}$) gives a new multi-handlebody and a new graph that we will denote $\text{cut}_D(\mathfrak{C})$ and $\text{cut}_D(\Gamma)$, respectively. The graph $\text{cut}_D(\Gamma)$ is obtained from Γ by replacing the intersection $\partial D \cap \Gamma$ by a pair of coupons colored by the morphisms $\sum_i x_i \otimes_{\mathbb{k}} y_i$ with $\{x_i\}_i$ a basis of $\text{Hom}_{\mathcal{H}\text{-mod}}(\mathbb{1}, P)$ and $\{y_i\}_i$ the dual basis of $\text{Hom}_{\mathcal{H}\text{-mod}}(P, \mathbb{1})$ with regards to the pairing $(x, y) \in \text{Hom}_{\mathcal{H}\text{-mod}}(\mathbb{1}, P) \times \text{Hom}_{\mathcal{H}\text{-mod}}(P, \mathbb{1}) \mapsto \tau_P(xy)$, where $P \in \text{Proj}_H$ is the projective element present on the intersection $\Gamma \cap \partial D$. The multi-handlebody $\text{cut}_D(\mathfrak{C})$ is obtained by cutting out a tubular open neighborhood of the disk D from \mathfrak{C} , i.e. $\text{cut}_D(\mathfrak{C}) = \mathfrak{C} \setminus (V(D))$ with $V(D) \simeq D \times]-\epsilon, \epsilon[$, for $\epsilon > 0$. We can see this operation represented in Figure 17.

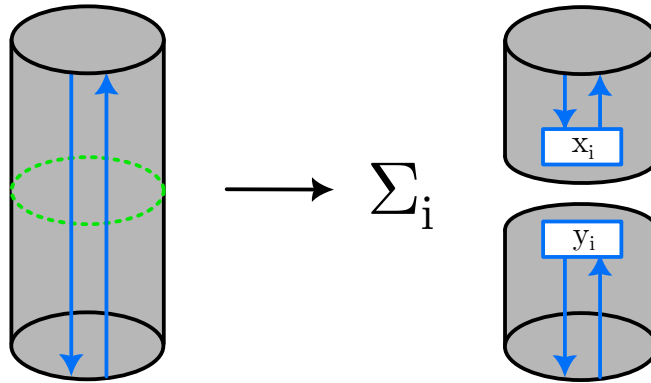


Figure 17: A cutting operation

Let M be a 3-dimensional connected oriented closed manifold and $M = \mathfrak{C}_\alpha \cup \mathfrak{C}_\beta$ be a Heegaard splitting of M . We denote by $(\Sigma_g, \alpha, \beta)$ the associated Heegaard diagram,

where α and β are sets of curves associated to the handlebodies \mathfrak{C}_α and \mathfrak{C}_β , respectively. Let us consider a ribbon graph $O_H \subset \Sigma \setminus (\alpha \cup \beta)$ defined as the braid closure on a disk of a coupon colored by $h \in \text{End}_{H\text{-mod}}(H)$ such that $F'(O_H) = 1$. We call Γ the bichrome diagram on the surface $\Sigma_g = \partial\mathfrak{C}_\alpha = \partial\mathfrak{C}_\beta$ formed by the set of curves β considered as red curves and the graph O_H mentioned above seen as the blue subgraph.

Theorem 4.21. [CGPMT20, Th. 2.4] *If (\mathfrak{C}, Γ) is a bichrome diagram obtained as described above from a 3-dimensional connected oriented closed manifold, then its image $F'(\mathfrak{C}, \Gamma) \in \mathbb{k}$ depends only on the diffeomorphism class of M . We can then define the chromatic spherical invariant $\mathcal{K}_{H\text{-mod}}$ by*

$$\mathcal{K}_{H\text{-mod}}(M) = F'(\mathfrak{C}, \Gamma).$$

Remark : If we cut along the α curves of a handlebody \mathfrak{C}_α associated to a Heegaard diagram $(\Sigma_g, \alpha, \beta)$, we notice that the multi-handlebody obtained is always connected (and diffeomorphic to B^3) because $\Sigma_g \setminus \alpha$ is connected.

The link between $\mathcal{K}_{H\text{-mod}}$ and the map F''_H is established by the following theorem.

Theorem 4.22. *Let M be a 3-dimensional connected oriented closed manifold and $(\Sigma_g, \alpha, \beta)$ be a Heegaard diagram of M . Let H be a spherical Hopf algebra and $H\text{-mod}$ the pivotal category of finite-dimensional H -modules. Then, for all standardized virtual Heegaard diagrams of the form $(\Sigma_g, \alpha, \beta, p_\infty, \gamma)$, we have*

$$\mathcal{K}_{H\text{-mod}}(M) = F''_H(\Sigma_g, \alpha, \beta, p_\infty, \gamma).$$

Proof. Let M be a 3-dimensional connected oriented closed manifold. Let us consider a Heegaard splitting $M = \mathfrak{C}_\alpha \cup \mathfrak{C}_\beta$ and an associated Heegaard diagram of M , $(\Sigma_g, \alpha, \beta)$. We will assume (potentially after performing an R_{II} move between the α and β curves) that, for every component $\alpha_i \in \alpha$, $\alpha_i \cap \beta \neq \emptyset$. We fix a point p_∞ in $\Sigma_g \setminus (\beta \cup \alpha)$ and a family of curves $\gamma \subset \Sigma_g \setminus \{p_\infty\}$ such that $(\Sigma_g, \alpha, \gamma, p_\infty, \gamma)$ is a standardized virtual Heegaard diagram. We once again consider a ribbon graph $O_H \subset \Sigma \setminus (\alpha \cup \beta)$ which is the braid closure in a disk of a coupon colored by $h \in \text{End}_{H\text{-mod}}(H)$ such that $F'(O_H) = 1$. We choose O_H on Σ such that there exists an open disk in Σ_g containing O_H , but not containing p_∞ , and such that $\gamma \cap O_H = \emptyset$. Unless stated otherwise, the following operations are skein relations between diagrams, and will be performed in the complement of an open disk containing the coupon colored by h . We will call this open disk V_h . Notably, the considered skein relations will always preserve the images under F' .

Let us consider, on the pointed surface $\Sigma_g \setminus p_\infty$, the bichrome diagram formed by the set of β curves, considered as red curves, and the graph O_H previously mentioned, considered as the blue subgraph. Through chromatic modifications with \vec{d} , we turn blue all β curves by connecting them with O_H (see Figure 18). We denote by $(\mathfrak{C}_\alpha, \Gamma)$ the bichrome diagram thus obtained. It is always possible (up to isotopy of the surface) to apply successive iterations of the chromatic modification, as shown in Figure 18, since the complement of $\Sigma_g \setminus \beta$ is connected.

We denote ψ a standard projection of $((\Sigma_g, \alpha, \gamma), p_\infty)$. We notice that Γ and β will have the same image by ψ except on an open disk containing the graph O_H and coupons colored by the chromatic morphism.

We use point 4 of Theorem 4.20 to cut $(\mathfrak{C}_\alpha, \Gamma)$ along disks D_i with curves α_i as boundaries. This gives us a new diagram on B^3 that we denote $\text{cut}(\Gamma)$. By definition, $\mathcal{K}_{H\text{-mod}}(M) = F'(B^3, \text{cut}(\Gamma))$.

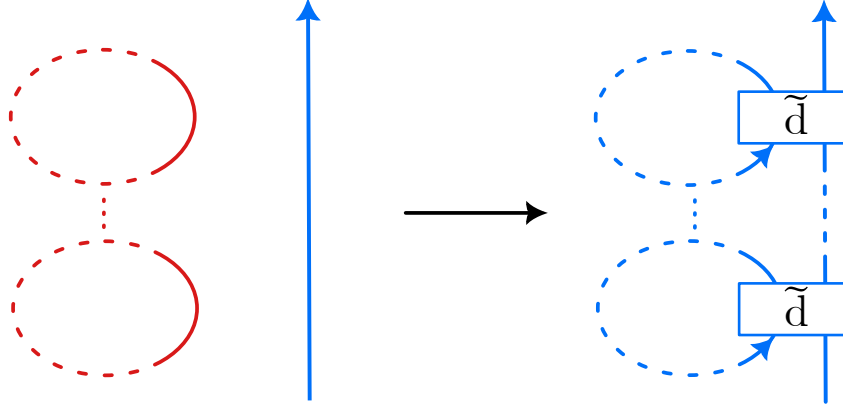


Figure 18: Transformation of a bichrome graph into an entirely blue graph with chromatic modifications

For all $i \in \{1, \dots, g\}$, cutting along a disk D_i creates two disks in the boundary of $cut_{D_i}(\mathcal{C}_\alpha)$. These disks boundaries, that we will call α_i^1 and α_i^2 , are connected by γ_i . Hence, the boundary of a tubular neighborhood T_i of $\alpha_i \cup \gamma_i$ (in $\partial(\mathcal{C}_\alpha)$) coincides with the boundary of a disk E_i in $\partial(cut_{D_i}(\mathcal{C}_\alpha))$. From now on, we consider a projection of $cut(\Gamma)$ onto the plane, identical to the projection ψ previously considered, except on the neighborhoods T_i and the inside of the disks E_i previously mentioned. The difference between the images of T_i and E_i by these two projections is represented in Figure 19 (image of T_i on the left and of E_i on the right).

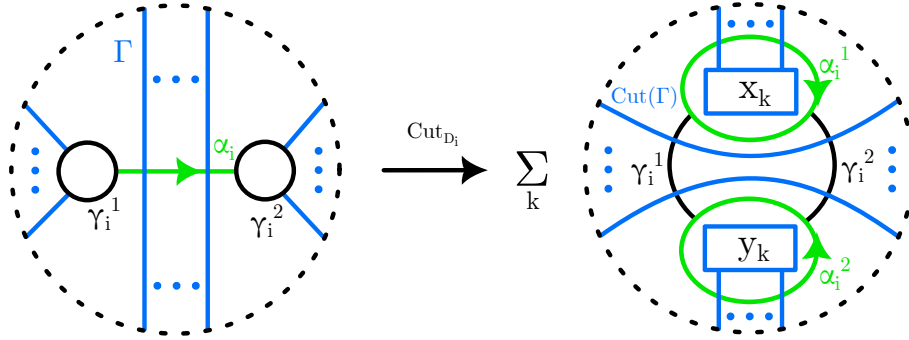


Figure 19: Projections onto the plane before and after cutting along a disk of boundary α_i

For the rest of the computation of $\mathcal{K}_{H\text{-mod}}$, we use graphical calculus in $\mathcal{V}ect_{\mathbb{k}}$: all edges are colored by the \mathbb{k} -space H , and, for all $h \in H$, the morphism $L_h : x \in H \mapsto hx$ is represented by a bead h . (i.e. both diagrams represented in Figure 20 are equivalent.) The evaluation and coevaluation morphisms in $H\text{-mod}$ and in $\mathcal{V}ect_{\mathbb{k}}$ differ by an action of g^d with $d \in \{-1, 0, 1\}$. Hence, we represent on the graph computed on $\mathcal{V}ect$ the beads $g^{\pm 1}$ corresponding to the maxima and minima of the graph (as shown in Figure 9).

In the open disk E_i , the two coupons of $cut(\Gamma)$ (x_k and y_k in Figure 19) are separated by the curves that were intersecting γ_i before the cutting. In $\mathcal{V}ect_{\mathbb{k}}$, Equality (1) shown

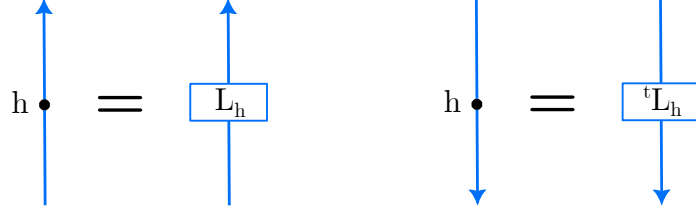


Figure 20: Relation between notation with bead and notation with coupons

in Figure 21 is verified. This equality is obtained thanks to the braiding τ of $\mathcal{V}ect$ (defined by $\tau : x \otimes y \in P \otimes P \mapsto y \otimes x$ with $P \in \text{Proj}_H$) represented by crossings in the figure. This enables us to express the morphism $\sum_k x_k \circ y_k = \Lambda_P$.

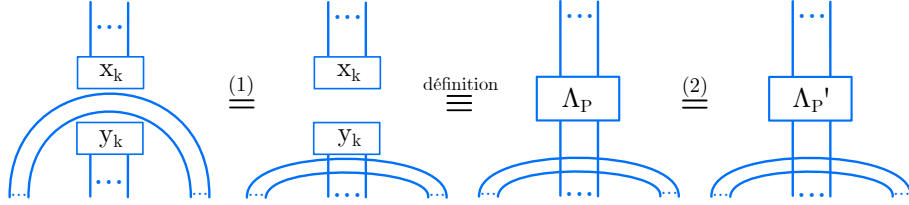


Figure 21: Relations between images by F' of diagrams in $\mathcal{V}ect_{\mathbb{k}}$

Lemma 4.23. [CGPMT20, Lemme 6.2] Let $\Lambda'_P : P \rightarrow P$ be the map determined by the action of the cointegral Λ over $P \in \text{Proj}_H$ (it is a H -module morphism due to H being unimodular, hence Λ is central). Let $\Lambda_P : P \rightarrow P$ be the morphism defined by $\Lambda_P = \sum_k x_k y_k$ with $\{x_k\}$ and $\{y_k\}$ the aforementioned dual bases. Then $\Lambda_P = \Lambda'_P$ for all projective module $P \in \text{Proj}_H$.

With Lemma 4.23 we can now "close" the curves where there are coupons $x_k \in \text{Hom}_{H\text{-mod}}(\mathbb{1}, P)$ and $y_k \in \text{Hom}_{H\text{-mod}}(P, \mathbb{1})$ following each other (see Equality (2) in Figure 21). We will again denote Γ the diagram obtained after the "closure" of the curves of $\text{cut}(\Gamma)$. We now see the cointegral's action $\Lambda \in H$ over the strands appear where the coupon was. In other words, on the set of these strands, we now place beads $\Lambda_{(j)}$ or $S(\Lambda_{(j)})$, as indicated in Figure 8.

Since the cutting has been performed along α curves, the resulting graph Γ has the same image under the projection onto the plane (therefore the same beads) as a flattening of β , except inside an open disk \mathcal{V} containing the graph \mathcal{O}_H and all coupons representing the chromatic morphism. From now on, when we will talk about "collected beads" on β , we will consider the beads obtained by this flattening of β . To end the proof, we will observe the parts of the diagrams contained inside the open disk \mathcal{V} .

Lemma 4.24. [CGPMT20, Lemme 6.6] For all $x \in H$ the following equality is verified in $\mathcal{V}ect_{\mathbb{k}}$

$$(\overline{ev}_H \otimes \text{Id}_H)(\text{Id}_{H^*} \otimes L_x \otimes \text{Id}_H)(\text{Id}_{H^*} \otimes \tilde{d})(\overline{coev}_H \otimes \text{Id}_H) = \lambda(gx) \text{Id}_H,$$

with $\overline{ev}_H : H^* \otimes H \rightarrow \mathbb{k}$ and $\overline{coev}_H : \mathbb{k} \rightarrow H^* \otimes H$ the evaluation and coevaluation maps in $\mathcal{V}ect_{\mathbb{k}}$.

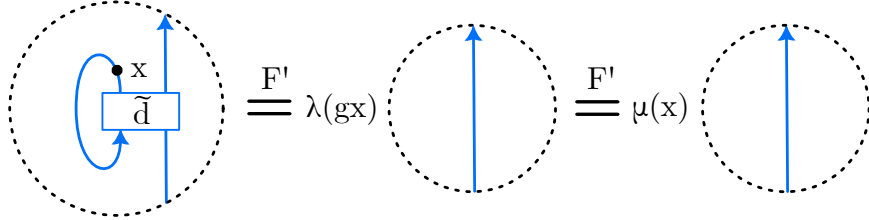
We notice here that the evaluation \overline{ev}_H and the coevaluation \overline{coev}_H are considered in $\mathcal{Vect}_{\mathbb{k}}$ and not with the spherical structure using the pivot g .

Proof. Let $\{e_i\}_i$ be a basis of H and $\{e_i^*\}_i$ be a dual basis of H^* . By developing the formulas for the evaluation and coevaluation in $\mathcal{Vect}_{\mathbb{k}}$ and the formula given for the chromatic morphism, for all $h \in H$ we have

$$\begin{aligned}
& (\overline{ev}_H \otimes \text{Id}_H)(\text{Id}_{H^*} \otimes L_x \otimes \text{Id}_H)(\text{Id}_{H^*} \otimes \tilde{d})(\overline{coev}_H \otimes \text{Id}_H)(h) \\
&= \sum_i (\overline{ev}_H \otimes \text{Id}_H)(\text{Id}_{H^*} \otimes L_x \otimes \text{Id}_H)(\text{Id}_{H^*} \otimes \tilde{d})(e_i^* \otimes e_i \otimes h) \\
&= \sum_i (\overline{ev}_H \otimes \text{Id}_H)(\text{Id}_{H^*} \otimes L_x \otimes \text{Id}_H)(e_i^* \otimes \lambda(S(h_{(1)})ge_i)h_{(2)} \otimes h_{(3)}) \\
&= \sum_i (\overline{ev}_H \otimes \text{Id}_H)(e_i^* \otimes \lambda(S(h_{(1)})ge_i)xh_{(2)} \otimes h_{(3)}) \\
&= \sum_i \lambda(S(h_{(1)})ge_i)e_i^*(xh_{(2)}) \otimes h_{(3)} \\
&= \lambda(S(h_{(1)})gxh_{(2)})h_{(3)} \\
&= \lambda(S^2(h_{(2)})S(h_{(1)})gx)h_{(3)} \\
&= \lambda(gx)\epsilon(h_{(1)})h_{(2)} \\
&= \lambda(gx)h.
\end{aligned}$$

The third-to-last equality comes from the sphericity of H . \square

Since $\lambda(gx) = \mu(x)$ by definition of μ , we can graphically represent in $\mathcal{Vect}_{\mathbb{k}}$ the lemma by



The equalities in the figure represent skein relations between images under F' of diagrams differing only on an open set as indicated.

Hence, for each coupon colored by the chromatic morphism on Γ , we obtain a scalar $\mu(b_i)$ with, for all $i \in \{1, \dots, g\}$, the product of the component's beads denoted $b_i \in H$. This product $b_i \in H$ is identical to the total bead b_i obtained on the corresponding component of β during the computation of F'' for a base point placed inside V . Indeed, we have seen previously that, outside the open set V , Γ has the same components and beads as those found on β during the computation F'' .

After applying Lemma 4.24 on each coupon colored by the chromatic morphism, we note that the image of graph Γ under F' is reduced to the image of graph O_H under F' multiplied by scalars $\mu(b_i)$. By definition of O_H and of F' , we find that $F'(\mathfrak{C}_\alpha, \Gamma) = \prod_{i \in \{1, \dots, g\}} \mu(b_i) F'(B^3, O_H) = \prod_{i \in \{1, \dots, g\}} \mu(b_i) = F''_H(\Sigma_g, \alpha, \beta, p_\infty, \gamma)$. Which gives us the desired result. \square

Since $\mathcal{K}_{H\text{-mod}}$ does not depend on the placement of point p_∞ , nor on the γ curves, Theorem 4.22 gives the following corollary.

Corollary 4.25. *Let M be a 3-dimensional connected oriented closed manifold and $(\Sigma_g, \alpha, \beta)$ be a Heegaard diagram of M . Let p_∞ be a point and γ be curves such that $(\Sigma_g, \alpha, \beta, p_\infty, \gamma)$ is a standardized virtual Heegaard diagram. Let H be a spherical Hopf algebra and $H\text{-mod}$ the pivotal category of finite-dimensional H -modules. The scalar $F''(\Sigma_g, \alpha, \beta, p_\infty, \gamma)$ does not depend on the choices of the point p_∞ or the curves γ .*

Consequently, for the rest of the article, we will allow ourselves to omit arguments p_∞ or γ in the map F'' when $(\Sigma_g, \alpha, \beta)$ is a non-virtual Heegaard diagram or a flattening of a non-virtual Heegaard diagram.

5 Relation between invariants

In this section, we fix H a spherical Hopf algebra on a field \mathbb{k} .

This section rests on a correspondence between specific Heegaard and surgery link diagrams. This approach is used and detailed in [CC19, Ch. 4] and [CW13, Ch. 3.1].

Theorem 5.1. [CC19, Th. 4.2][BP79, Th. 4.1 & Th.4.2] *Any 3-dimensional oriented closed manifold M admits a Heegaard diagram $D = (\Sigma_g, \alpha, \beta)$, with some genus g , verifying the following properties:*

- *There exists a collection of g curves $\gamma = \{\gamma_1, \dots, \gamma_g\}$ on Σ_g such that $D_1 = (\Sigma_g, \gamma, \beta)$ and $D_2 = (\Sigma_g, \alpha, \gamma)$ are diagrams of S^3 verifying $[\gamma \cap \beta] = \text{Id}_g$ and $[\alpha \cap \gamma] = \text{Id}_g$.*
- *If we see β as a framed link in S^3 , where S^3 is determined by D_1 , and where framing is chosen as a parallel copy of β in the Heegaard surface, then β is a surgery link of M .*

The idea behind the proof in [BP79, Theorem 4.1 and Theorem 4.2] is to use a surgery presentation of M by a link $L \subset \mathbb{R}^2 \times \mathbb{R}^- \subset S^3$ that we will consider as the flat closure of a pure braid. We can then "untangle" that link in such a way that the only strands of L not resting in the plane $\mathbb{R}^2 \times \{0\}$ are unknotted arcs with trivial framing.

We will now describe a way to see the β curves of a Heegaard diagram verifying the hypotheses of Theorem 5.1 as a link in \mathbb{R}^3 . This perspective is based on the reasoning inside the proof mentioned above, which is why the link obtained will be the one mentioned in the theorem.

Let $(\Sigma_g, \alpha, \beta)$ be a Heegaard diagram of a (3-dimensional oriented closed) manifold M and $\gamma \subset \Sigma_g$ be a collection of curves such as described in Theorem 5.1. Therefore, there exists a point $p_\infty \in \Sigma_g \setminus (\alpha \cup \beta)$ such that $(\Sigma_g, \alpha, \beta, p_\infty, \gamma)$ is a standardized virtual Heegaard diagram, with changes of the orientation of certain curves of γ if necessary. Let us consider ψ a standard projection of $(\Sigma_g, \alpha, \beta, p_\infty, \gamma)$. We will see a way to visualize the image $\psi(\beta) \subset \mathbb{R}^2$ as a link in \mathbb{R}^3 (the following explanations are illustrated in Figure 22). Let r_θ be the rotation with radius θ around axis $\{\frac{3}{2}\} \times \mathbb{R} \times \{0\}$ (counterclockwise). For all $i \in \{1, \dots, g\}$, the image $r_{[0, \pi]}(D_i^1) = \{r_\theta(D_i^1) | \theta \in [0, \pi]\}$ describes an unknotted handle with trivial framing and attaching region $\{D_i^1 \cup D_i^2\}$, attached to $\mathbb{R}^2 \times \mathbb{R}^+$. The image of $\psi(\beta) \cap \gamma_i^1$ by the set of rotations $r_{[0, \pi]}$ is a strand in the boundary

of the handle thus defined, which connects $\psi(\beta) \cap \gamma_i^1$ and $\psi(\beta) \cap \gamma_i^2$. The strands thus defined correspond to the unknotted arcs with trivial framing mentioned in the idea behind the proof of Theorem 5.1. Therefore, we obtain a link $\psi(\beta) \cup_{1 \leq i \leq g} r_{[0, \pi]}(\psi(\beta) \cap \gamma_i^1)$ in $\mathbb{R}^3 \subset \mathbb{S}^3$ which is, in particular, a surgery link of the manifold M (see proof of [BP79, Theorem 4.1 and Theorem 4.2]).

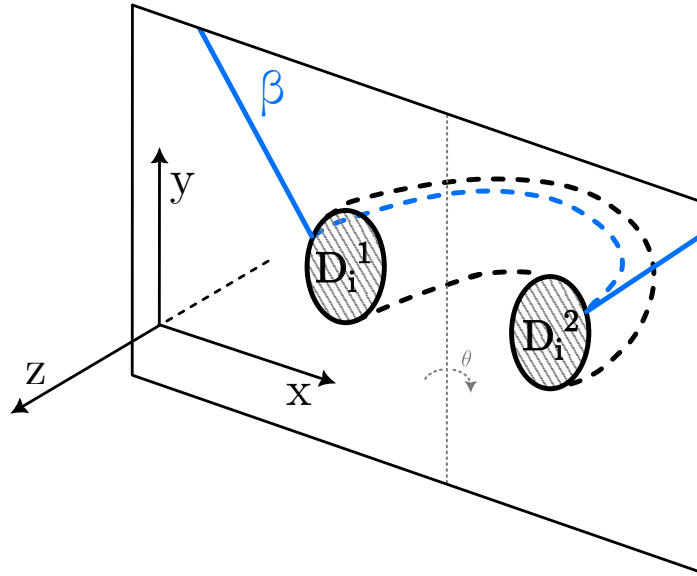


Figure 22: Visualization of the image of a standard projection in \mathbb{R}^3

Remark : In the rest of this article, we will represent the image of a Heegaard diagram $D \subset \mathbb{R}^2 \subset \mathbb{R}^3$ by a standard projection on \mathbb{R}^2 , and an associated surgery link $L \subset \mathbb{R}^3 \subset \mathbb{S}^3$ as shown in Figure 23. Outside the open disks represented in the figure, it follows from the above that the link L can be projected onto the plane (with the same standard projection), and we can note that we obtain the same curves for the projection of the Heegaard diagram and for the associated surgery link seen in the plane.

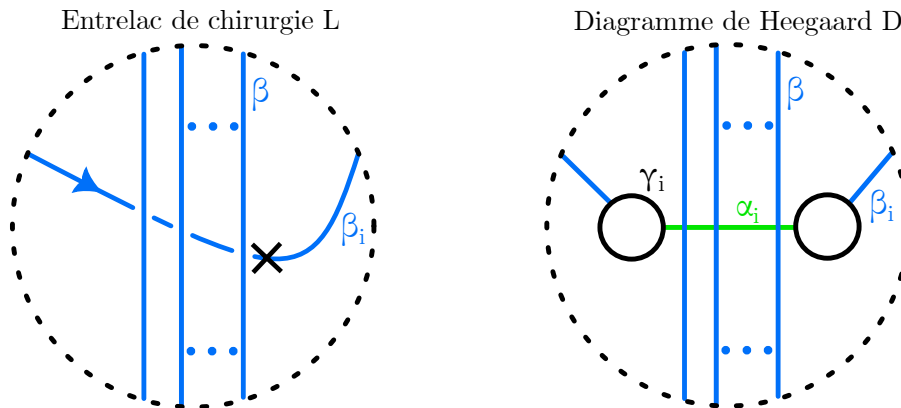


Figure 23: Heegaard diagram and surgery link of the same manifold M

This similarity between diagrams allows us to see the following relation between the spherical chromatic invariant $\mathcal{K}_{H\text{-mod}}$ and the renormalized Hennings-Kauffman-Radford invariant $\text{HKR}_{D(H)}$ of M .

Theorem 5.2 (Main theorem). *Let H be a spherical Hopf algebra and M be a 3-dimensional connected oriented closed manifold. We have*

$$\mathcal{K}_{H\text{-mod}}(M) = \text{HKR}_{D(H)}(M)$$

with $D(H)$ the Drinfeld double of H .

Remark : We suspect to be true the following, more general, version of this theorem,

$$\mathcal{K}_{\mathcal{C}}(M) = \text{HKR}_{Z(\mathcal{C})}(M)$$

with \mathcal{C} a spherical category and $Z(\mathcal{C})$ its Drinfeld center.

Proof. Let H be a spherical Hopf algebra and M be a 3-dimensional connected oriented closed manifold.

By Theorem 5.1, there exists a Heegaard diagram and a surgery link representing the manifold M and respecting the assumptions of that theorem (we have seen that these diagrams will have analogous forms).

We can assume (potentially by adding R_{II} moves between α and β curves) that, for all $i \in \{1, \dots, g\}$, the intersection $\alpha_i \cap \beta$ is non-empty.

Therefore, on one hand, we have $D = (\Sigma_g, \alpha, \beta)$, a Heegaard diagram of M along with a point p_∞ and a collection of curves γ such that $(\Sigma_g, \alpha, \beta, p_\infty, \gamma)$ is standardized, and that $[\gamma \cap \beta] = \text{Id}_g$. We will compute the bichrome invariant $\mathcal{K}_{H\text{-mod}}^2(M)$ with this diagram. On the other hand, we have L , a surgery link of M originating from the β curves. We will compute the invariant $\text{HKR}_{D(H)}(M)$ with that link.

Each component β_i of L , $i \in \{1, \dots, g\}$, contains a "horizontal" segment included in any neighborhood (on the plane) of the curve α_i (because $[\gamma \cap \beta] = \text{Id}_g$ and $[\gamma \cap \alpha] = \text{Id}_g$). Hence, we can consider that each component β_i is oriented in such a way that this horizontal segment of β_i will be oriented from left to right. Indeed, if it is not the case for a given curve β_i , we can reverse its orientation without changing the image of the invariants, since HKR is invariant under orientation reversal of any curve β_i (the same is true for \mathcal{K} by Proposition 4.17).

On each component β_i , we will choose to place the base points on the right of all crossings of this horizontal strand, and before any extremum on β_i (see the left in Figure 23).

We will seek to make explicit $\text{HKR}_{D(H)}(M)$. We know, by results of Part 2.2, that we can express elements of $D(H)$ with those of H and H^* . Hence, Lemma 5.3 will allow us to express $\text{HKR}_{D(H)}(M)$ with elements of H (and H^*).

We start by paying attention to the beads placed on crossings during the computation of the HKR invariant. Each crossing gives two beads that will be collected in different orders during their multiplication.

Remark : We denote the R -matrix of $D(H)$ by $R^D = \sum_i r_i^D \otimes s_i^D$ (or by $R^D = r_i^D \otimes s_i^D$, implying the summation). Therefore, we will talk about an s bead (resp. an r bead) for beads colored by elements s_i^D (resp. r_i^D) with $n \in \mathbb{Z}$ of the R -matrix (see Figure 1). We will also talk about g beads for beads colored by $g \in H$, $g^D \in D(H)$ or their inverse.

What follows can be visualized on the left side of Figure 24.

We notice that s beads will always follow each other on that horizontal segment, without g bead in between. Conversely, r beads will always be on "vertical" segments and can have g beads between them.

For each crossing, we associate a pair of indices $(i, h) \in \mathbb{Z}^2$. Index i is the index of the undercrossing component. Here, it is also the horizontal component. If we order the crossings from the base point, following orientation on β_i , this crossing is the h -th one among the undercrossings of component β_i . We denote by k_i the number of under-crossings of component β_i and g is the total number of components (we recall that $g \in \mathbb{N}$ is also the genus of the associated Heegaard diagram of M determined in Theorem 5.1).

We will denote $s_{i,h}^D$ and $r_{i,h}^D$ the elements coloring the beads of the crossing (i, h) , and $d_{i,h} \in \mathbb{Z}$ the exponent of the antipode applied to $r_{i,h}^D$.

We recall that, by definition (see Figure 1), $d_{i,h}$ depends on the orientation of β at the crossing. Hence, we have

$$d_{i,h} = \begin{cases} 0 & \text{if the vertical } \beta \text{ curve is downward,} \\ -1 & \text{else.} \end{cases}$$

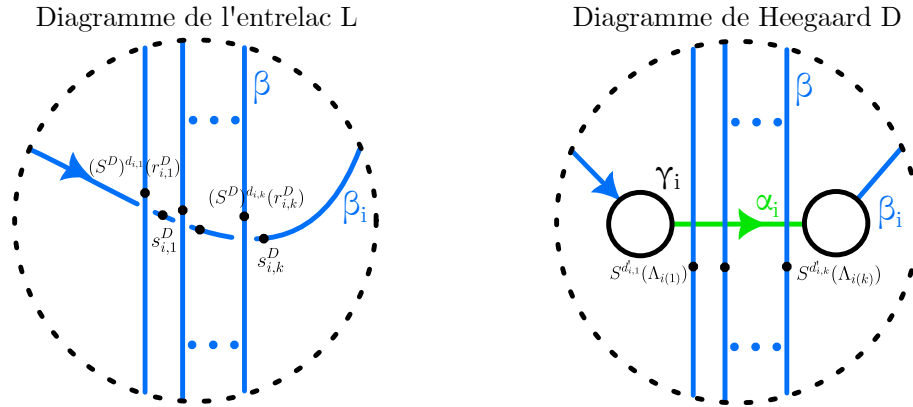


Figure 24: Beads from crossings on L and on D

For each crossing, we can associate a second pair of indices $(j, v) \in \mathbb{N}^2$ with j the index of the overcrossing component (which here is also the vertical component), and, if we order overcrossings from the base point, following orientation on the component, this crossing is the v -th among the overcrossings of component j . We denote by l_j the number of overcrossings of the component j . This allows us to define the map ϕ by $\phi(j, v) = (i, h)$. That map associates the component and collection order of an r bead to the component and collection order of the s bead from the same crossing. For example, in the case represented in Figure 26, we will have $\phi(1, 1) = (2, 1)$, $\phi(1, 2) = (1, 1)$, $\phi(2, 1) = (2, 3)$, $\phi(2, 2) = (2, 2)$ and $\phi(2, 3) = (1, 2)$. We will sometimes denote $\phi(j, v) = (p_{j,v}, q_{j,v})$ when we will need to refer independently to the components of the pair.

Remark : Since the studied Hopf algebras are non-commutative, we will denote

$$\overrightarrow{\prod}_{m \in (n, \dots, 1)} a_i = a_n a_{n-1} \cdots a_1$$

to stress the order of the elements in a product.

The total bead collected on each component i during the computation of the HKR invariant is

$$s_{i, k_i}^D \cdots s_{i, 1}^D \left(\overrightarrow{\prod}_{m \in (l_i, \dots, 1)} (g^D)^{n_{i,m}} (S^D)^{d_{\phi(i,m)}} (r_{\phi(i,m)}^D) \right) (g^D)^{n_{i,0}}$$

with $n_{i,m}$ the algebraic sum of the exponents of all g beads between the bead colored by $r_{\phi(i,m)}^D$ and the next r or s bead (or between the base point and the first r bead in the case of $n_{i,0}$). See Figures 25 and 26 for an example illustrating this formula.

With the beads thus collected, the formula of HKR gives

$$\text{HKR}_{D(H)}(M) = (\delta^D)^{-s} \overrightarrow{\prod}_{i=1}^{\mathfrak{g}} \mu^D \left(s_{i, k_i}^D \cdots s_{i, 1}^D \left(\overrightarrow{\prod}_{m \in (l_i, \dots, 1)} (g^D)^{n_{i,m}} (S^D)^{d_{\phi(i,m)}} (r_{\phi(i,m)}^D) \right) (g^D)^{n_{i,0}} \right)$$

where s is the signature of the linking matrix of the link. We will show in Lemma 5.3 that this expression can be reformulated with elements from H , which gives us

$$\text{HKR}_{D(H)}(M) = \delta^{-s} \overrightarrow{\prod}_{i=1}^{\mathfrak{g}} \mu \left(\left(\overrightarrow{\prod}_{m \in (l_i, \dots, 1)} g^{n_{i,m}} S^{d_{\phi(i,m)}+1} (\Lambda_{\mathcal{P}_{i,m}(q_{i,m})}) \right) g^{n_{i,0}} \right).$$

Let us now return to the computation of $\mathcal{K}_{H\text{-mod}}(M)$. During the computation of this invariant, a single bead is associated to each crossing between α_i and β_j (see Figure 8).

Due to the correspondence between the crossing of the Heegaard diagram D and those of the surgery link L , we can use the map ϕ as seen above. For each crossing, the map ϕ associates to a pair of indices (j, v) the pair (i, h) with j, i, v and h integers defined as follows. Here, j is the index of the component β_j on which the bead will be placed and i is the index of the component α_i involved in the crossing. If we order the beads along β_j , starting at the base point and following the orientation, then this bead is the v -th one collected on β_j . If we order the crossings on α_i from left to right, then this crossing is the h -th one among the crossings on α_i .

The total bead collected on each component i in the Heegaard diagram D is given by

$$g^{n'_{i, l_i}} S^{d_{\phi(i, l_i)}+1} (\Lambda_{\phi(i, l_i)}) \cdots S^{d_{\phi(i, 1)}+1} (\Lambda_{\phi(i, 1)}) g^{n'_{i, 0}},$$

with $d_{i,m} \in \{-1, 0\}$ and $n_{i,m}$ the exponents previously seen for all $i \in \{1, \dots, \mathfrak{g}\}$ and all $m \in \{1, \dots, l_i\}$. Indeed, by definition of beads on crossings (see Figures 1 and 8), we note that we recover the exponents $d_{i,m} + 1$ on the antipodes. Furthermore, since we chose analogous forms for L and D , we know that we have the same minima, maxima, and crossings (in amount and orders) on both. Hence, $n_{i,m}$ is also the algebraic sum of

exponents on g beads between the bead colored by $S^{d_{\phi(i,m)}+1}(\Lambda_{\phi(i,m)})$ (or the base point if $m = 0$) and the next bead that is not a g bead (or the base point if $m = l_i$).

Therefore, by Theorem 4.22, we find the following formula for $\mathcal{K}_{H\text{-mod}}(M)$.

$$\mathcal{K}_{H\text{-mod}}(M) = \epsilon(\Lambda)^v \prod_{i=1}^g \mu \left(\left(\overrightarrow{\prod}_{m \in (l_i, \dots, 1)} g^{n_{i,m}} S^{d_{\phi(i,m)}+1}(\Lambda_{\phi(i,m)}) \right) g^{n_{i,0}} \right),$$

where $v = 0$, hence $\epsilon(\Lambda)^v = 1$ because we assumed earlier that any α curve intersects the set β . See Figures 25 and 27 for an example illustrating this formula.

If we apply Lemma 5.3 to the expressions we have for the invariants, we can conclude that

$$\text{HKR}_{D(H)}(L) = (\delta^D)^{-s} \mathcal{K}_{H\text{-mod}}(D).$$

Hence, proving that $\delta^D = 1$ (which will be done in Lemma 5.4) allows us to directly conclude the expected result $\text{HKR}_{D(H)}(M) = \mathcal{K}_{H\text{-mod}}(M)$.

To finish the proof, all that is left is to prove the two lemmas announced above.

Lemma 5.3. *Let us consider a spherical algebra H and its double $D(H)$ with the notations previously introduced and from Part 2.2.*

We then have the equality

$$\begin{aligned} & \prod_{b=1}^g \mu^D \left(s_{i_b, k_b}^D \cdots s_{i_b, 1}^D \left(\overrightarrow{\prod}_{m \in (l_b, \dots, 1)} (g^D)^{n_{b,m}} (S^D)^{d_{\phi(b,m)}} (r_{i_{\phi(b,m)}}^D) \right) (g^D)^{n_{b,0}} \right) \\ &= \prod_{b=1}^g \mu \left(\left(\overrightarrow{\prod}_{m \in (l_b, \dots, 1)} g^{n_{b,m}} S^{d_{\phi(b,m)}+1}(\Lambda_{p_{b,m}, (q_{b,m})}) \right) g^{n_{b,0}} \right), \end{aligned}$$

with, for all $(i, j) \in \mathbb{N}^2$, $\Lambda_{p_{i,j}, (q_{i,j})}$ the $q_{i,j}$ -nth factor in the coproduct $\Delta^{(l_{p_{i,j}})}(\Lambda_{p_{i,j}})$ (cointegral associated to the component $p_{i,j}$).

Proof. Let (e_1, \dots, e_n) be a basis of H and (e_1^*, \dots, e_n^*) be a dual basis of $H^{*\text{cop}}$, we recall that we may make explicit the R -matrix of $D(H)$ by

$$R^D := \sum_{i=1}^n (e \otimes e_i) \otimes (e_i^* \otimes 1_H).$$

Thus, we have

$$\begin{aligned}
& \prod_{b=1}^g \mu^D \left(s_{i_{b,k_b}}^D \cdots s_{i_{b,1}}^D \left(\overrightarrow{\prod}_{m \in (l_b, \dots, 1)} (g^D)^{n_{b,m}} (S^D)^{d_{\phi(b,m)}} (r_{i_{\phi(b,m)}^D}^D) \right) (g^D)^{n_{b,0}} \right) \\
& \stackrel{(1)}{=} \prod_{b=1}^g (\Lambda \otimes \mu) \left((e_{i_{b,k_b}}^* \otimes 1_H) \cdots (e_{i_{b,1}}^* \otimes 1_H) \right. \\
& \quad \left. \left(\overrightarrow{\prod}_{m \in (l_b, \dots, 1)} (\epsilon \otimes g)^{n_{b,m}} (\epsilon \otimes S^{d_{\phi(b,m)}}(e_{i_{\phi(b,m)}})) \right) (\epsilon \otimes g)^{n_{b,0}} \right) \\
& \stackrel{(2)}{=} \prod_{b=1}^g (\Lambda \otimes \mu) \left(e_{i_{b,k_b}}^* \cdots e_{i_{b,1}}^* \otimes \left(\overrightarrow{\prod}_{m \in (l_b, \dots, 1)} g^{n_{b,m}} S^{d_{\phi(b,m)}}(e_{i_{\phi(b,m)}}) \right) g^{n_{b,1}} \right) \\
& \stackrel{(3)}{=} \prod_{b=1}^g e_{i_{b,k_b}}^* (\Lambda_{b,(1)}) \cdots e_{i_{b,1}}^* (\Lambda_{b,(k_b)}) \mu \left(\left(\overrightarrow{\prod}_{m \in (l_b, \dots, 1)} g^{n_{b,m}} S^{d_{\phi(b,m)}}(e_{i_{\phi(b,m)}}) \right) g^{n_{b,0}} \right) \\
& \stackrel{(4)}{=} \prod_{b=1}^g \mu \left(\left(\overrightarrow{\prod}_{m \in (l_b, \dots, 1)} g^{n_{b,m}} S^{d_{\phi(b,m)}}(\Lambda_{p_{b,m},(l_b - q_{b,m} + 1)}) \right) g^{n_{b,0}} \right) \\
& \stackrel{(5)}{=} \prod_{b=1}^g \mu \left(\left(\overrightarrow{\prod}_{m \in (l_b, \dots, 1)} g^{n_{b,m}} S^{d_{\phi(b,m)} + 1}(\Lambda_{p_{b,m},(q_{b,m})}) \right) g^{n_{b,0}} \right).
\end{aligned}$$

Equality (1) is obtained by expressing the elements of $D(H)$ with elements of H according to the formulas from Part 2.2.

Due to the expression for multiplication in the double, for all $f, f' \in H^{*,\text{cop}}$, and all $x, x' \in H$, we have

$$(f \otimes x)(f' \otimes x') = f f' \otimes x x' \quad \text{if } x = 1_H \text{ or } f' = \epsilon.$$

Which gives equality (2).

Equality (3) is the application of $\Lambda \otimes \mu$ to elements of $D(H)$. We distinguish here g copies of Λ , a copy Λ_i being associated to each component β_i .

By a property of the dual basis, for all $x \in H$, and $f \in H^*$ then $\sum_i e_i^*(x) f(e_i) = f(x)$, which gives equality (4).

Equality (5) is obtained by the relation $S(\Lambda) = \Lambda$.

□

Lemma 5.4. *Let H be a spherical Hopf algebra with pivot g and $D(H)$ be its Drinfeld double with the notations introduced in Part 2.2. Then $\delta^D := \mu^D(g^D \theta^D) = 1$, with $\theta^D := \sum_i s_i^D g^D r_i^D$.*

Proof. Since H is spherical, we can apply Proposition 2.14 and express elements of

$D(H)$ with elements of H .

$$\begin{aligned}
 \delta^D &= \mu^D(g^D \theta^D) = \mu^D(g^D \sum_i s_i^D g^D r_i^D) = \sum_i \mu^D(g^D s_i^D g^D r_i^D) \\
 &= \sum_i (\Lambda \otimes \mu)((e_i^* \otimes 1_H)(\epsilon \otimes g)(\epsilon \otimes e_i)(\epsilon \otimes g)) \\
 &= \sum_i (\Lambda \otimes \mu)(e_i^* \otimes g e_i g) \\
 &= \sum_i e_i^*(\Lambda) \otimes \mu(g e_i g) \\
 &= \mu(g^2 \Lambda) = \epsilon(g)^3 \lambda(\Lambda) = 1
 \end{aligned}$$

□

Remark : Here it is essential for $D(H)$ to be ribbon and unimodular (because quasitriangular and spherical) to be able to express g^D with g .

This concludes the proof of Theorem 5.2.

□

Example :

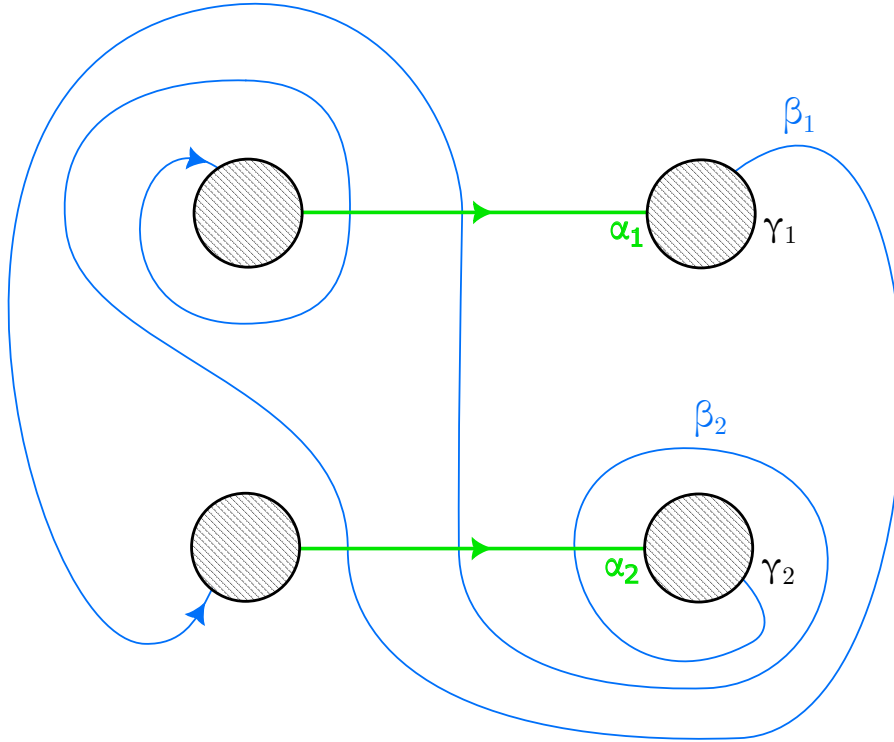


Figure 25: Heegaard diagram of the manifold \mathbb{S}^3

Applied to the diagram in Figure 25, the process described in part 3 to compute the

invariant $\text{HKR}_{D(H)}$ (see Figure 26) gives the scalar

$$S_{\text{HKR}} = \mu^D(s_{1,2}^D s_{1,1}^D g^D r_{1,1}^D g^D (S^D)^{-1}(r_{2,1}^D)) \\ \mu(s_{2,3}^D s_{2,2}^D s_{2,1}^D (S^D)^{-1}(r_{1,2}^D) (S^D)^{-1}(r_{2,2}^D) g^D (S^D)^{-1}(r_{2,3}^D)) \in \mathbb{k}.$$

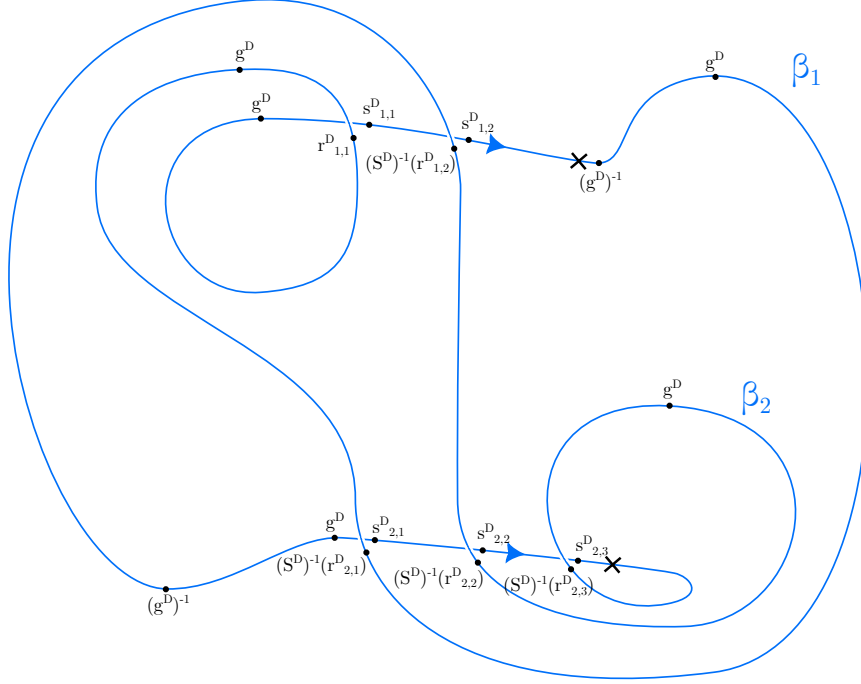


Figure 26: Surgery link associated to the virtual diagram represented in Figure 27

Applied to the diagram in Figure 25, the process described in part 4.2 to compute the invariant $\mathcal{K}_{\text{H-mod}}$ (see Figure 27) gives the scalar

$$S_{\mathcal{K}} = \mu(gS(\Lambda_{1,(1)})g\Lambda_{2,(1)})\mu(\Lambda_{1,(2)}\Lambda_{2,(2)}g\Lambda_{2,(3)}) \in \mathbb{k}.$$

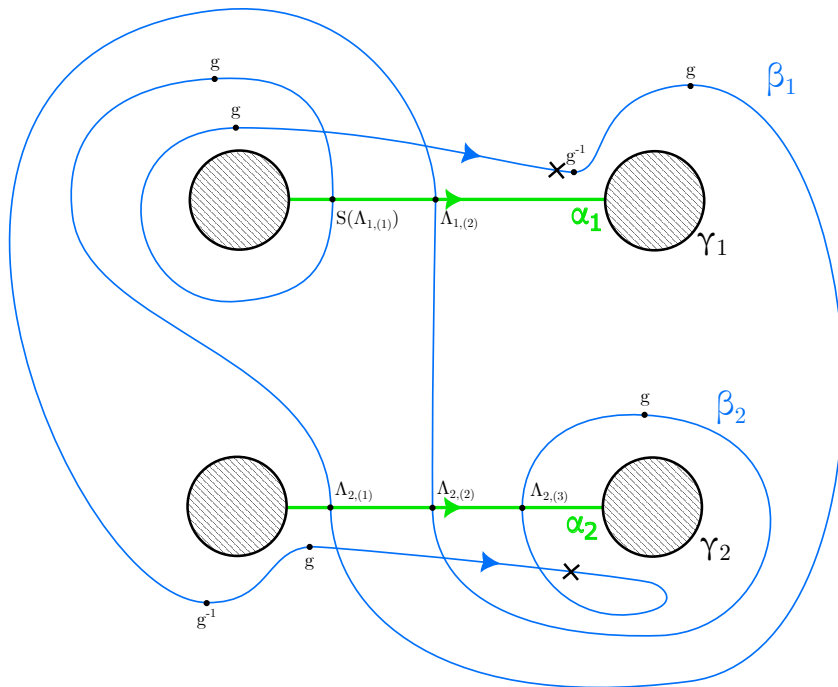


Figure 27: Flattening of the diagram represented in Figure 25

6 References

- [Art25] Emil Artin. Theorie der zöpfe. In *Abhandlungen aus dem mathematischen Seminar der Universität Hamburg*, volume 4, pages 47–72. Springer, 1925.
- [BBG21] Anna Beliakova, Christian Blanchet, and Azat M Gainutdinov. Modified trace is a symmetrised integral. *Selecta Mathematica*, 27(3):31, 2021.
- [Bir74] Joan S Birman. *Braids, links, and mapping class groups*. Number 82. Princeton University Press, 1974.
- [BP79] Joan S Birman and Jerome Powell. Special representations for 3-manifolds. In *Geometric topology*, pages 23–51. Elsevier, 1979.
- [CC19] Liang Chang and Shawn X Cui. On two invariants of three manifolds from Hopf algebras. *Advances in Mathematics*, 351:621–652, 2019.
- [CGHPM23] Francesco Costantino, Nathan Geer, Benjamin Haïoun, and Bertrand Patureau-Mirand. Skein $(3+1)$ -tqfts from non-semisimple ribbon categories. *arXiv preprint arXiv:2306.03225*, 2023.
- [CGPMT20] Francesco Costantino, Nathan Geer, Bertrand Patureau-Mirand, and Vladimir Turaev. Kuperberg and Turaev–Viro invariants in unimodular categories. *Pacific Journal of Mathematics*, 306(2):421–450, 2020.
- [CGPMV23] Francesco Costantino, Nathan Geer, Bertrand Patureau-Mirand, and Alexis Virelizier. Non compact $(2+1)$ -tqfts from non-semisimple spherical categories. *arXiv preprint arXiv:2302.04509*, 2023.
- [CW13] Liang Chang and Zhenghan Wang. $|Z_{Kup}|=|Z_{Henn}|^2$ for lens spaces. *Quantum Topology*, 4(4):411–445, 2013.
- [DRGG⁺22] Marco De Renzi, Azat M Gainutdinov, Nathan Geer, Bertrand Patureau-Mirand, and Ingo Runkel. 3-dimensional tqfts from non-semisimple modular categories. *Selecta Mathematica*, 28(2):42, 2022.
- [GHPM22] Nathan Geer, Ngoc-Phu Ha, and Bertrand Patureau-Mirand. Modified symmetrized integral in g -coalgebras. *arXiv preprint arXiv:2209.04691*, 2022.
- [GPMV13] Nathan Geer, Bertrand Patureau-Mirand, and Alexis Virelizier. Traces on ideals in pivotal categories. *Quantum Topol*, 4(1):91–124, 2013.
- [Hen96] Mark Hennings. Invariants of links and 3-manifolds obtained from Hopf algebras. *J. London Math. Soc. (2)*, 54(3):594–624, 1996.
- [Kas95] Christian Kassel. *Quantum Groups*. 1995.
- [KR95] Louis H Kauffman and David E Radford. Invariants of 3-manifolds derived from finite dimensional hopf algebras. *Journal of knot theory and its ramifications*, 4(01):131–162, 1995.
- [Lau14] François Laudenbach. A proof of reidemeister-singer’s theorem by cerf’s methods. In *Annales de la Faculté des sciences de Toulouse: Mathématiques*, volume 23, pages 197–221, 2014.

- [MSWY23] Lukas Müller, Christoph Schweigert, Lukas Woike, and Yang Yang. The lyubashenko modular functor for drinfeld centers via non-semisimple string-nets. *arXiv preprint arXiv:2312.14010*, 2023.
- [OS04] Peter Ozsváth and Zoltán Szabó. An introduction to heegaard floor homology. *Floer homology, gauge theory, and low-dimensional topology*, 5:3–27, 2004.
- [Rad11] David E Radford. *Hopf algebras*, volume 49. World Scientific, 2011.
- [Rei33] Kurt Reidemeister. Zur dreidimensionalen topologie. In *Abhandlungen aus dem Mathematischen Seminar der Universität Hamburg*, volume 9, pages 189–194. Springer, 1933.
- [Sin33] James Singer. Three-dimensional manifolds and their heegaard diagrams. *Transactions of the American Mathematical Society*, 35(1):88–111, 1933.
- [Tur10] Vladimir G Turaev. *Quantum invariants of knots and 3-manifolds*. de Gruyter, 2010.
- [TV17] Vladimir G Turaev and Alexis Virelizier. *Monoidal categories and topological field theory*, volume 322. Springer, 2017.